Planck and B-mode missions:
robustness, implications for inflation, and near-term prospects

William C. Jones
Princeton University

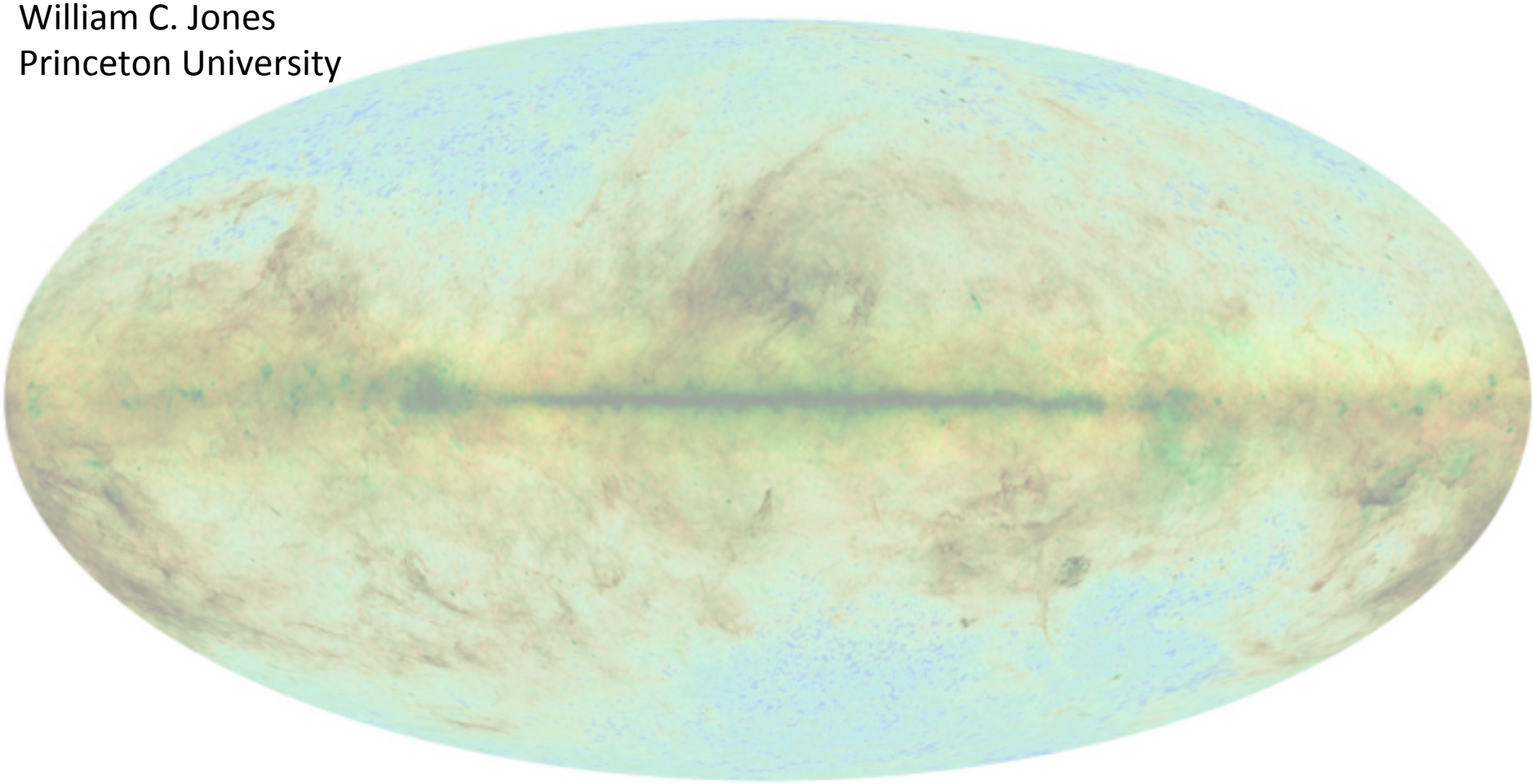

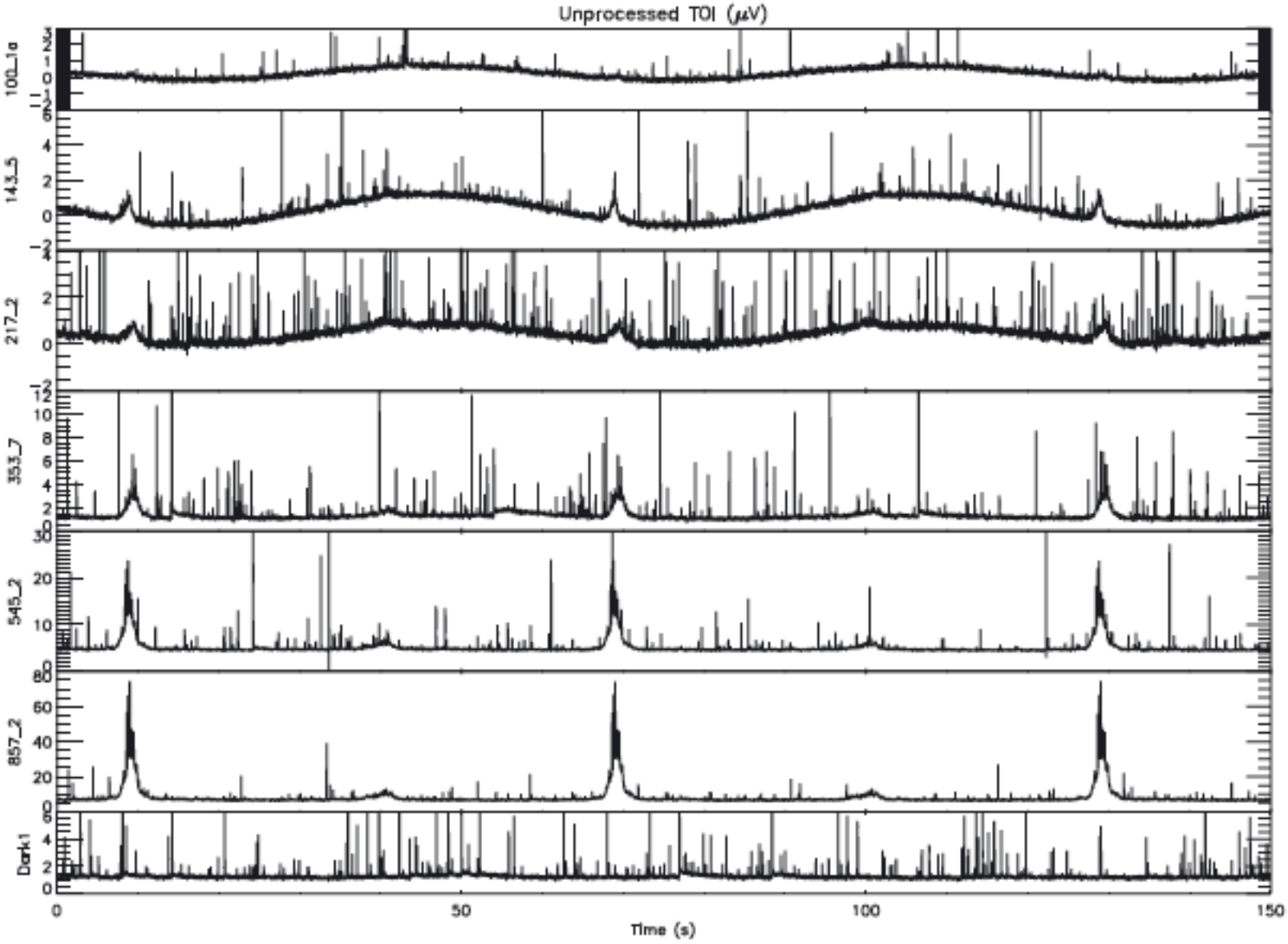
Unprocessed TOI (μV)
100_1a
143_5
217_2
353_7
545_2
857_2
Dark1
0
50
100
150
Time (s)

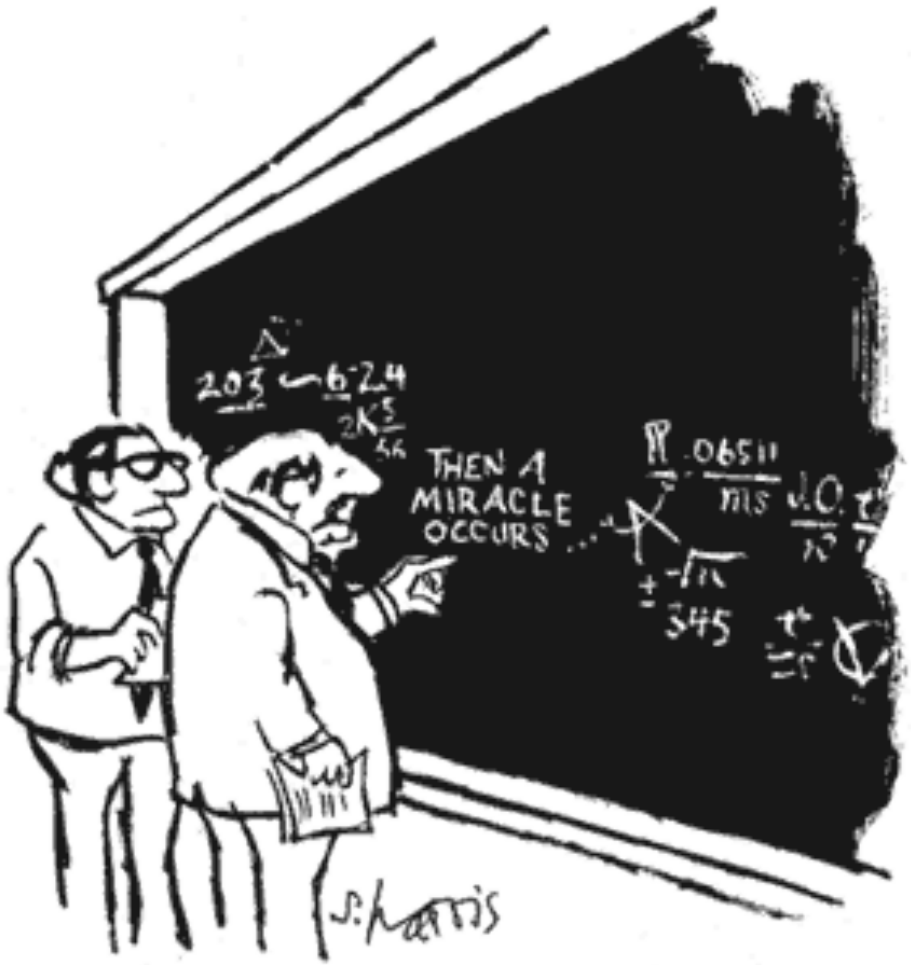

"I THINK YOU SHOULD BE MORE EXPLICIT HERE IN STEP TWO."

Sidney Harris (2006)

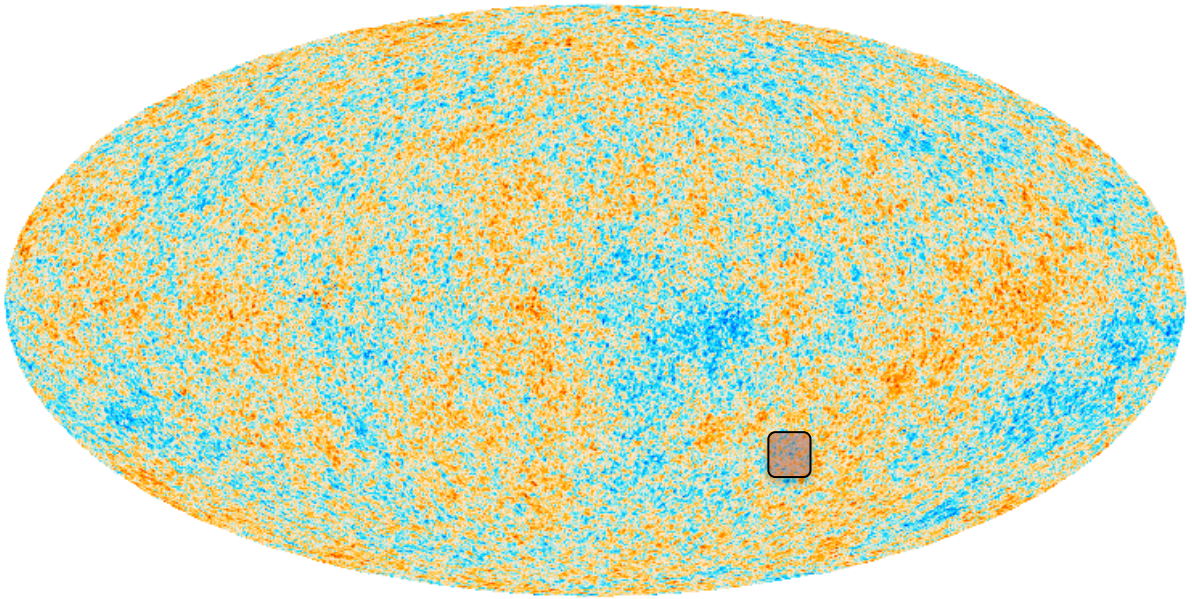
−500
500 μK_{CMB}

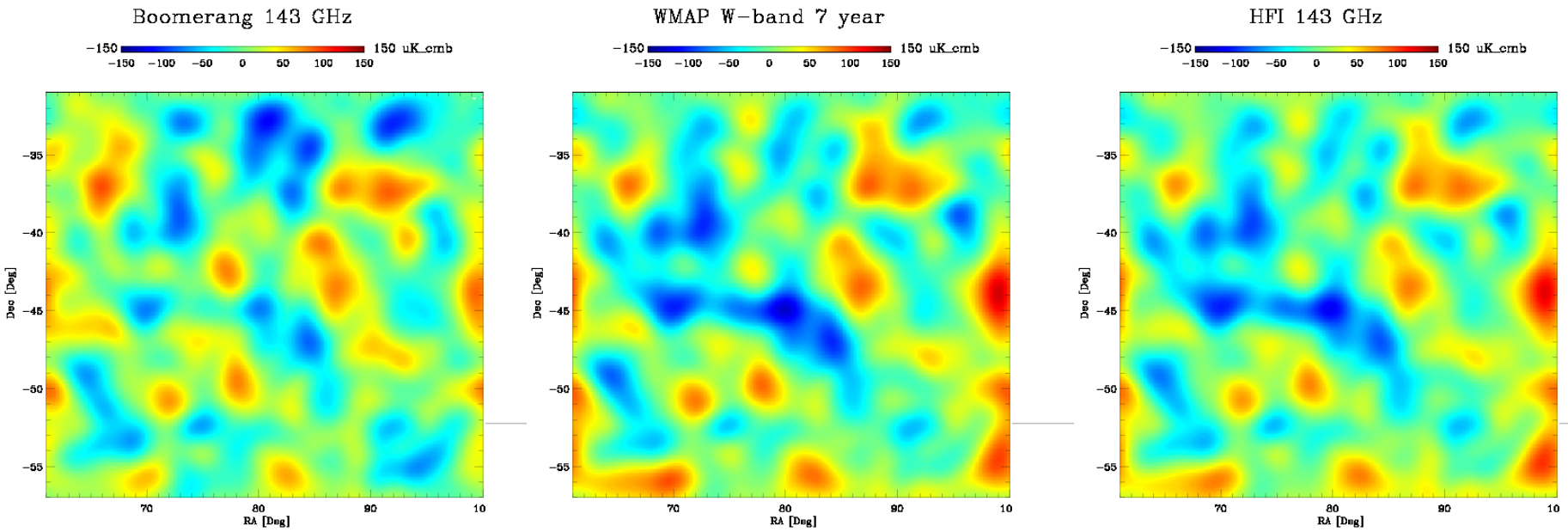
Boomerang 143 GHz
WMAP W−band 7 year
HFI 143 GHz
−150
150 uK_cmb
−150 −100 −50 0 50 100 150
Dec [Deg]
RA [Deg]
−35
−40
−45
−50
−55
70
80
90
10

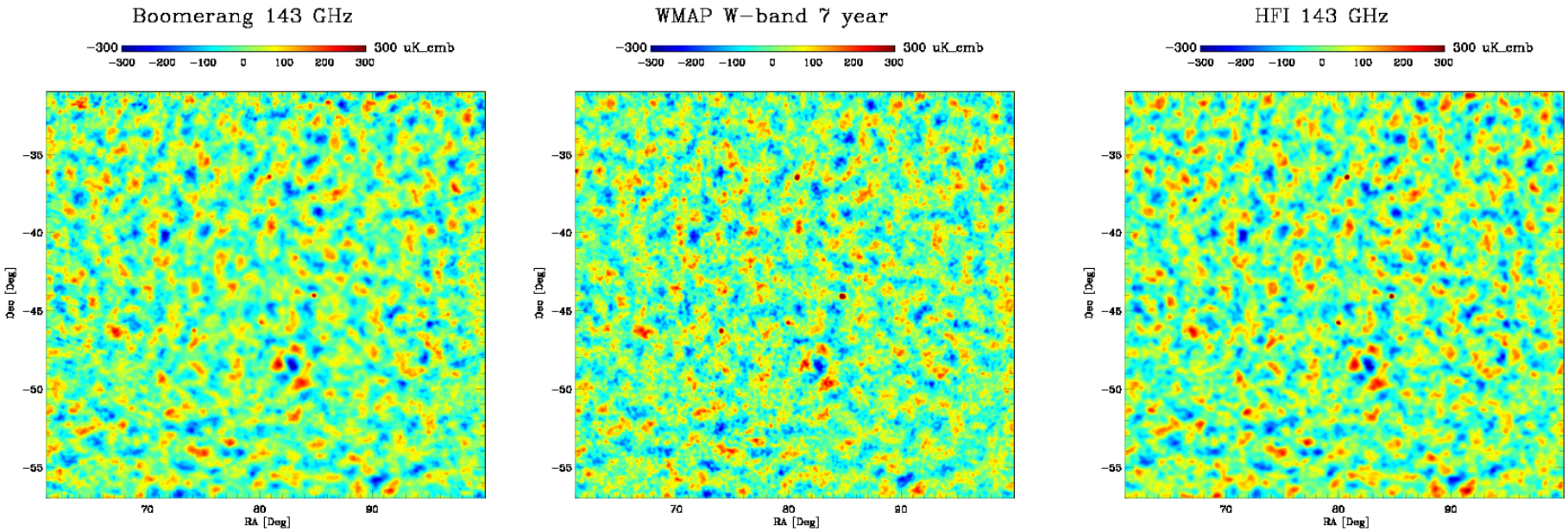
Boomerang 143 GHz
−300 300 uK_cmb
−300 −200 −100 0 100 200 300
WMAP W−band 7 year
−300 300 uK_cmb
−300 −200 −100 0 100 200 300
HFI 143 GHz
−300 300 uK_cmb
−300 −200 −100 0 100 200 300
Dec [Deg]
−35
−40
−45
−50
−55
70
80
90
RA [Deg]

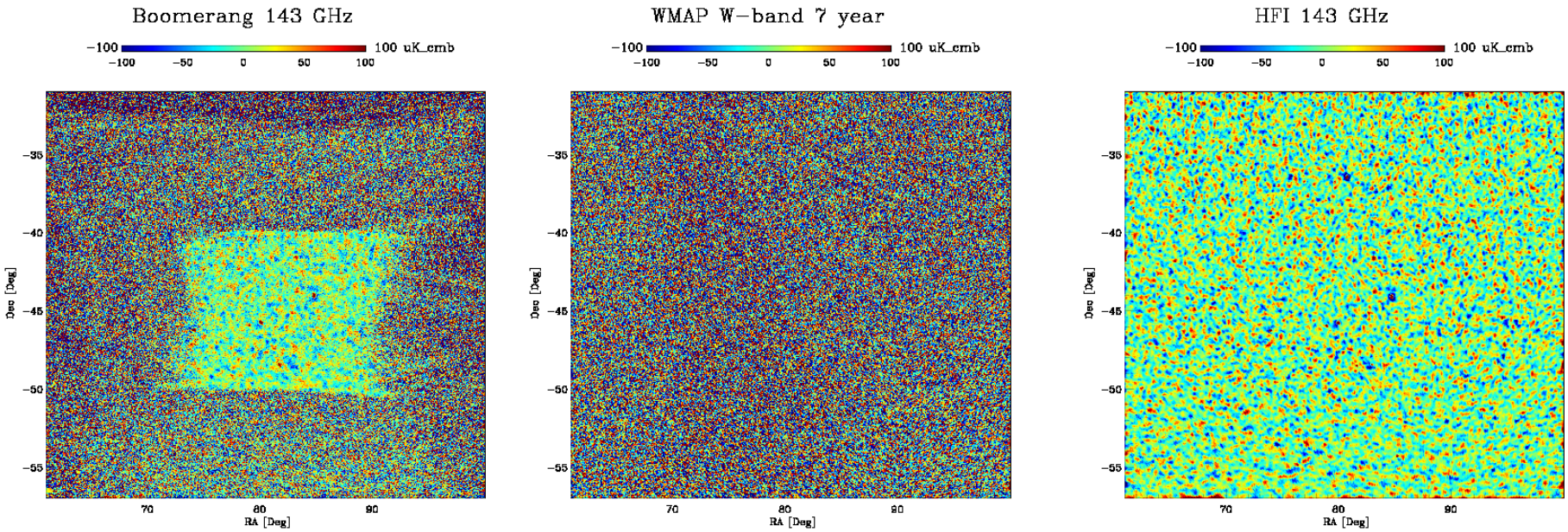
Boomerang 143 GHz
−100 100 uK_cmb
−100 −50 0 50 100
WMAP W−band 7 year
−100 100 uK_cmb
−100 −50 0 50 100
HFI 143 GHz
−100 100 uK_cmb
−100 −50 0 50 100
Dec [Deg]
−35
−40
−45
−50
−55
70
80
90
RA [Deg]

Cosmic Concordance.

Cosmic Concordance.

Cosmic Concordance.

Cosmic Concordance.

(across more than three orders of magnitude in scale!)

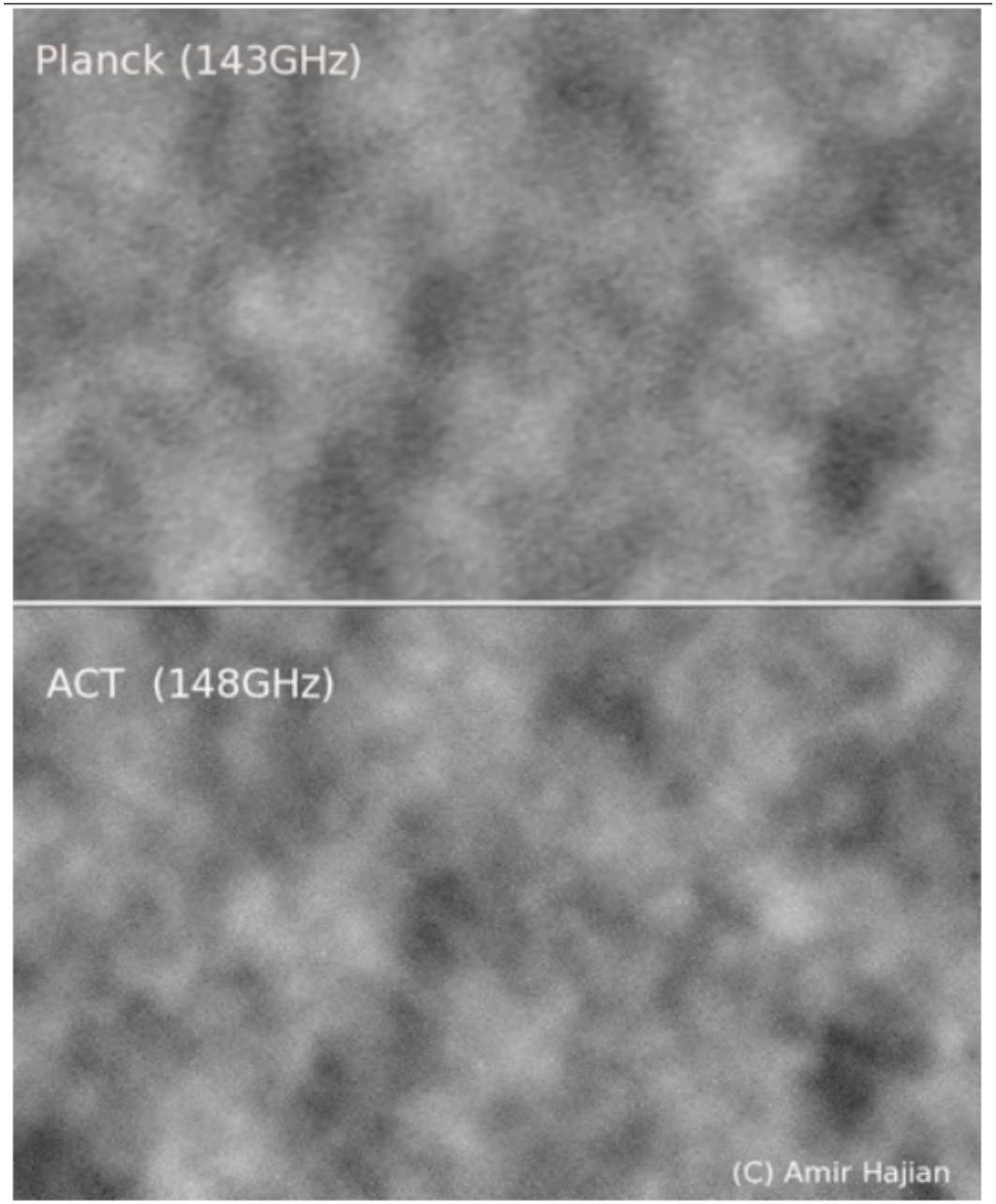

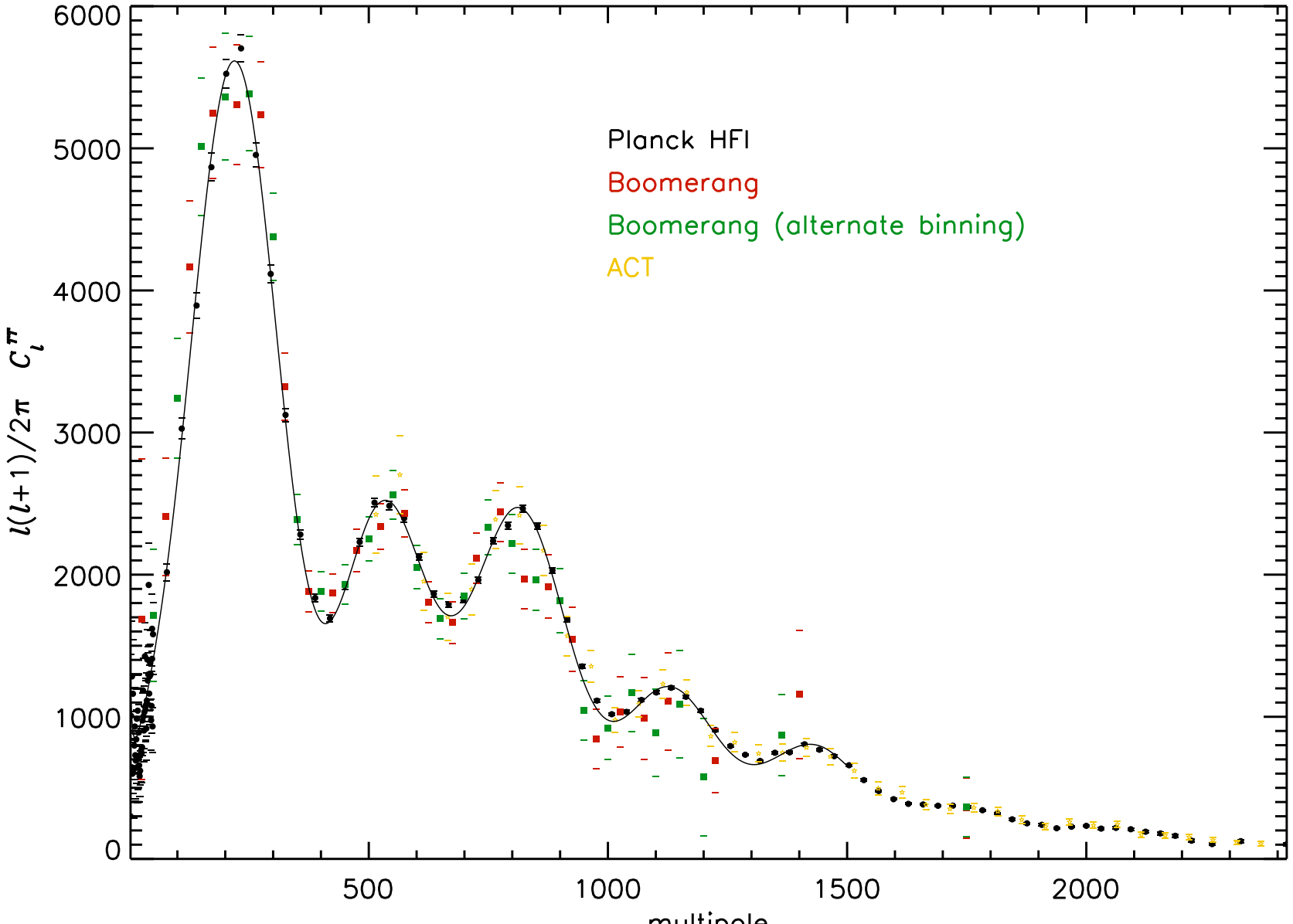
Planck HFI
Boomerang
Boomerang (alternate binning)
ACT
$l(l+1)/2\pi \ C_l^{TT}$
multipole
0
1000
2000
3000
4000
5000
6000
500
1000
1500
2000

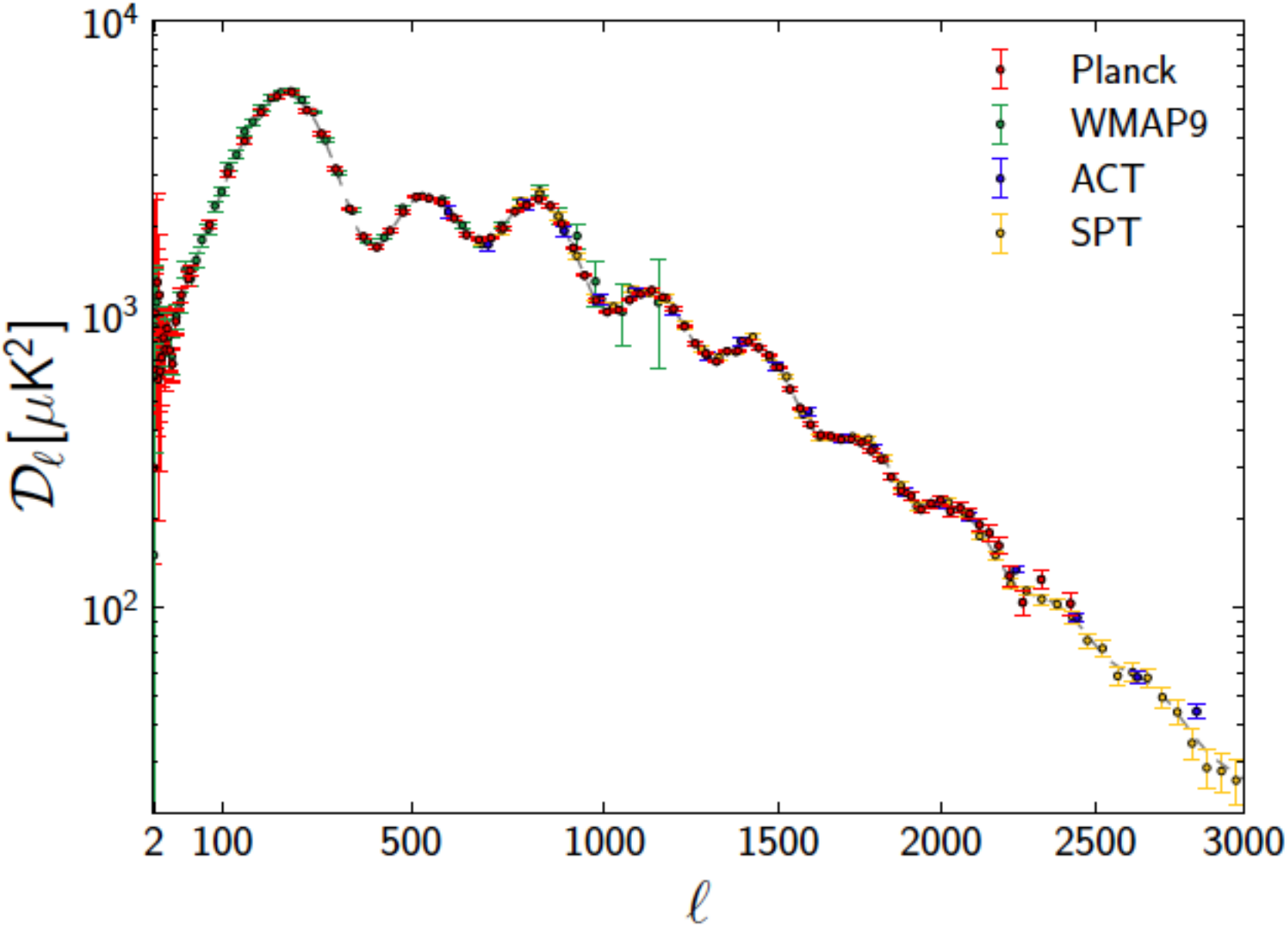
10^4
10^3
10^2
$\mathcal{D}_\ell\,[\mu K^2]$
Planck
WMAP9
ACT
SPT
2
100
500
1000
1500
2000
2500
3000
ℓ

The standard flat, six-parameter, ΛCDM model successfully describes the Planck temperature and lensing-potential power spectra at multipoles $\ell > 40$.

No evidence of deviation from power-law, adiabatic, scalar fluctuations

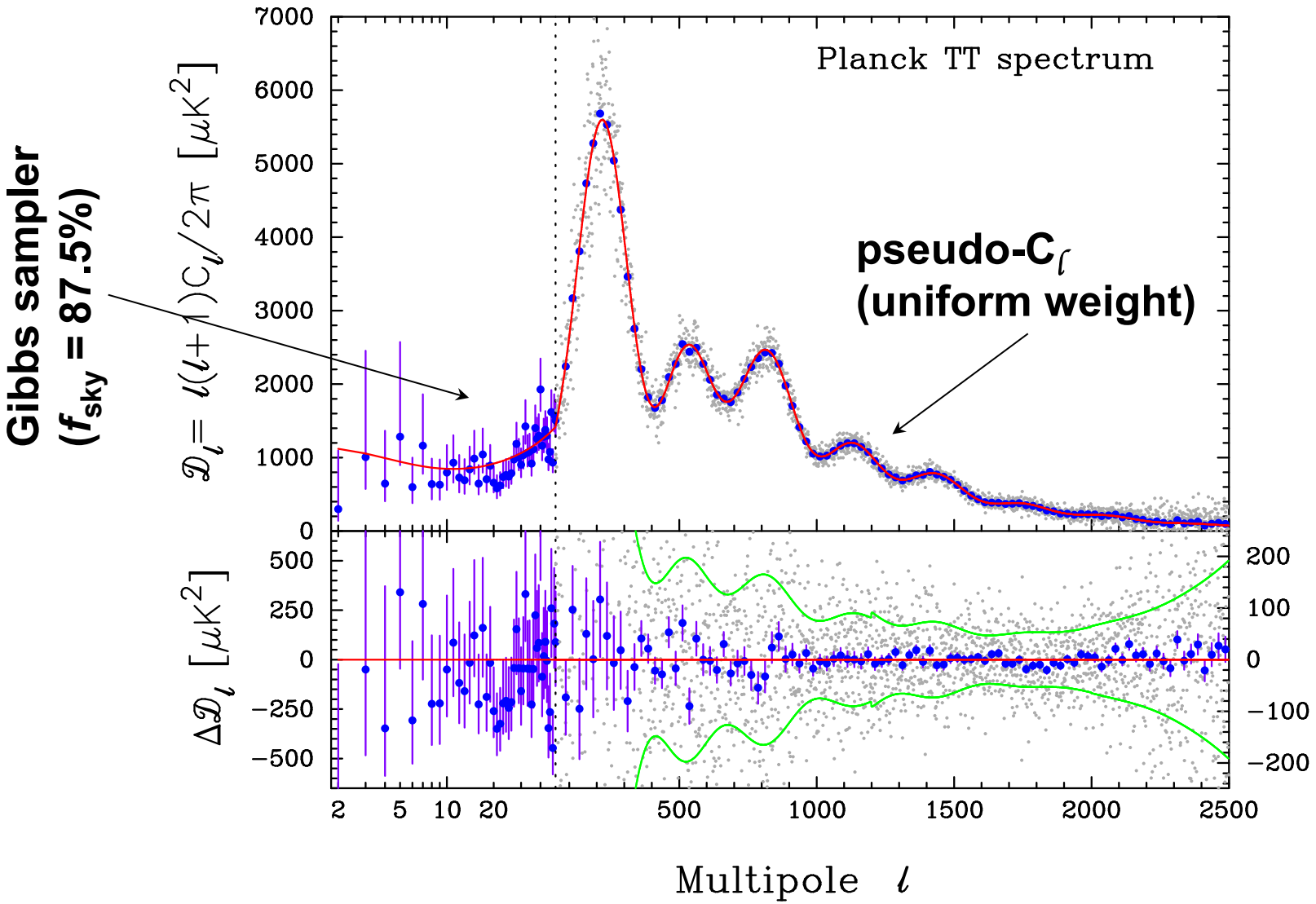

Cosmological Summary:

- ΛCDM best fit driven by $80 < \ell < 2000$
- lensing breaks the geometric degeneracy (both lensed C_ℓ^{TT}, $C_\ell^{\varphi\varphi}$)
- ↑ baryons, ↑ dark matter, ↓ cosmological const.
- *excellent* agreement with BBN, BAO acoustic scale
- scale invariance ($n_s < 1$) ruled out at 5.4 sigma (CMB alone)
- low H_0 relative to HST
- no evidence for (data disfavor)
  - anything beyond the 3 standard neutrino species
  - curvature, running index, dynamical dark energy, isocurvature, sterile neutrinos, …
  - local type NG, $f_{NL} < 6$ or so.
- above multipole of 40, excellent agreement with ΛCDM
- below multipole of 40, the χ^2 doesn't tell the story…
- complicated disagreement with WMAP on the CMB

FOUR-YEAR *COBE*[1] DMR COSMIC MICROWAVE BACKGROUND OBSERVATIONS: MAPS AND BASIC RESULTS

C. L. Bennett,[2] A. J. Banday,[3] K. M. Górski,[3] G. Hinshaw,[3] P. Jackson,[3] P. Keegstra,[3]
A. Kogut,[3] G. F. Smoot,[4] D. T. Wilkinson,[5] and E. L. Wright[6]

Received 1996 January 11; accepted 1996 March 21

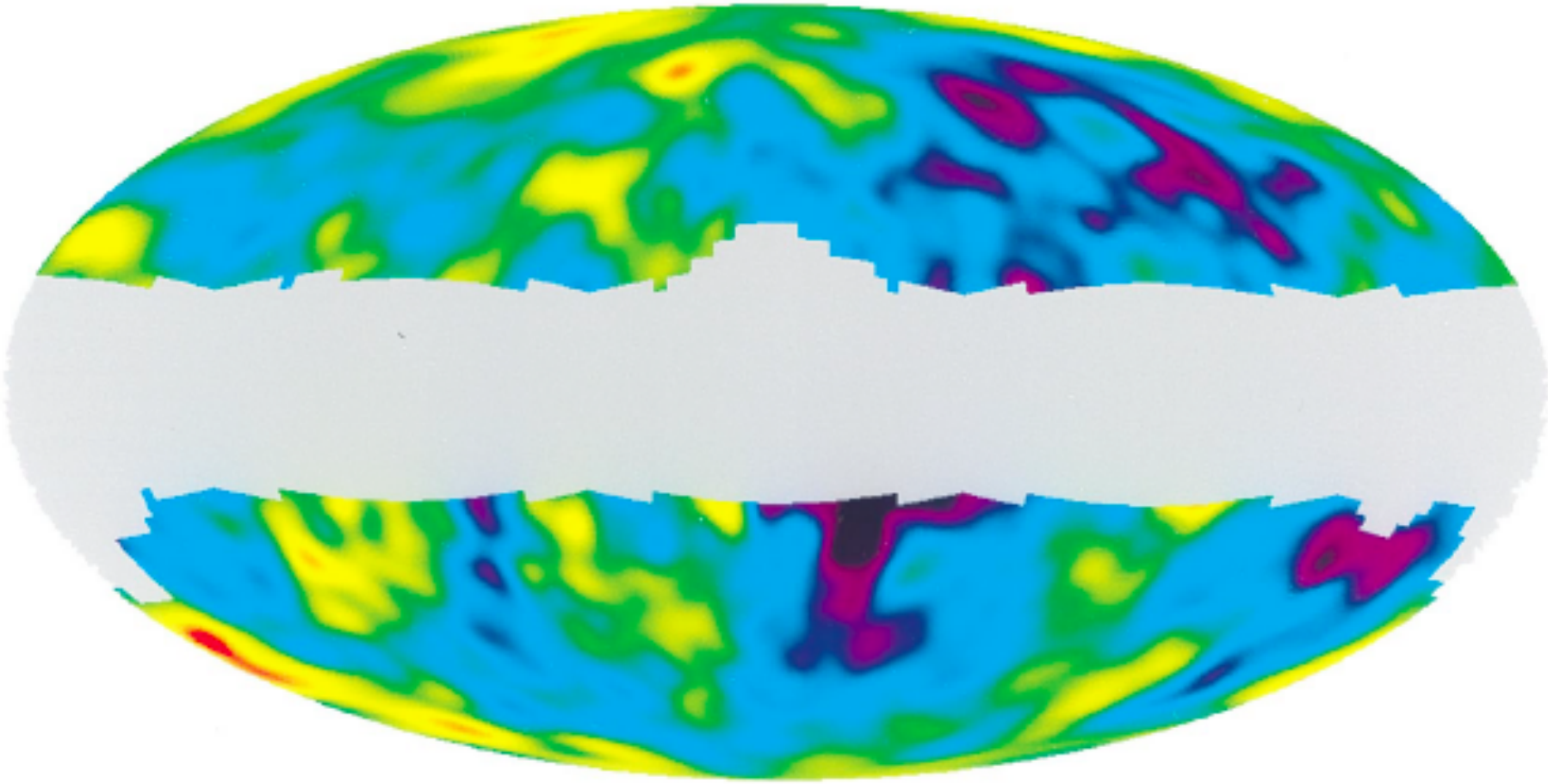

The lensing potential according to *Planck*

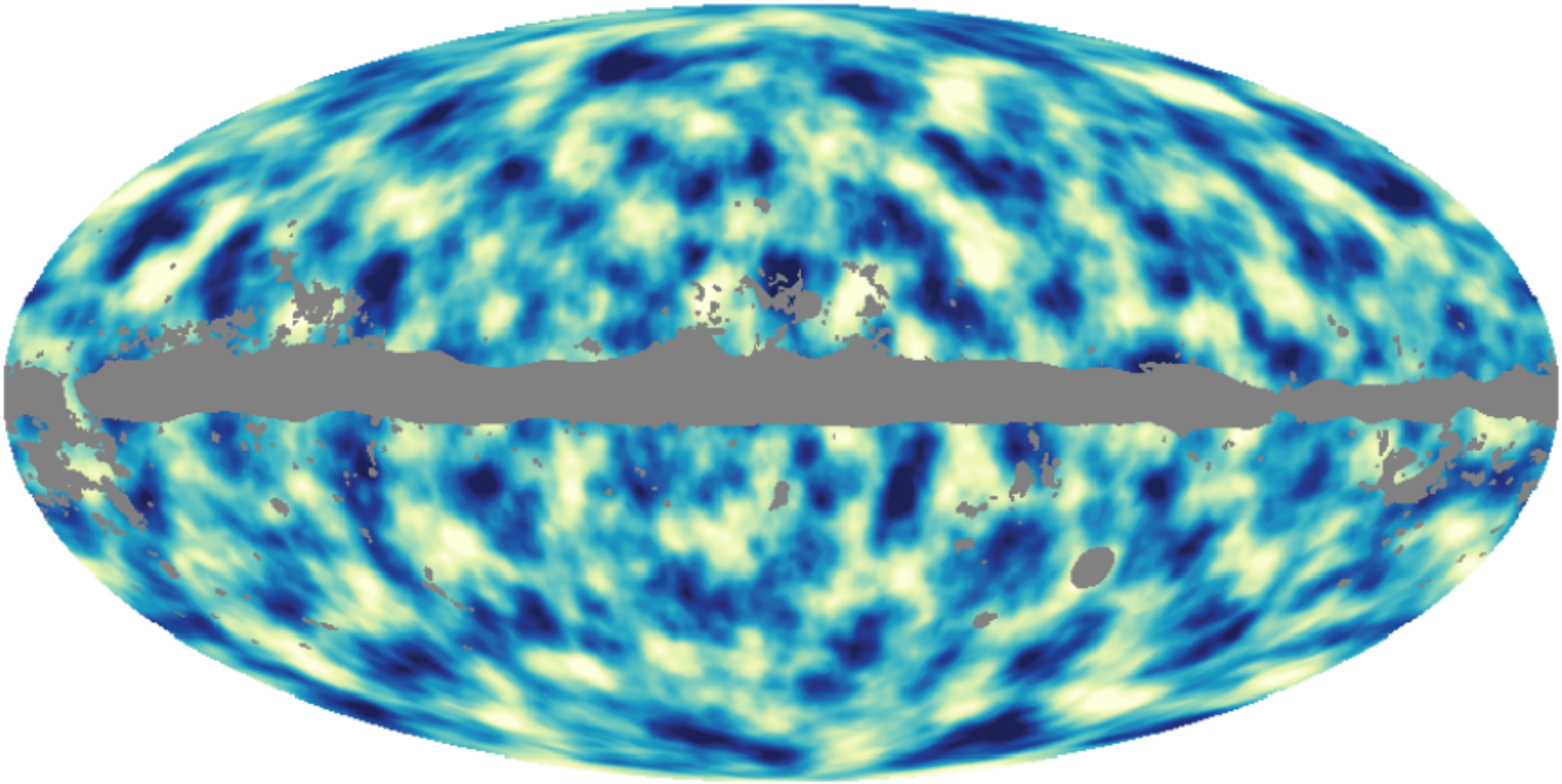

The lensing power spectrum

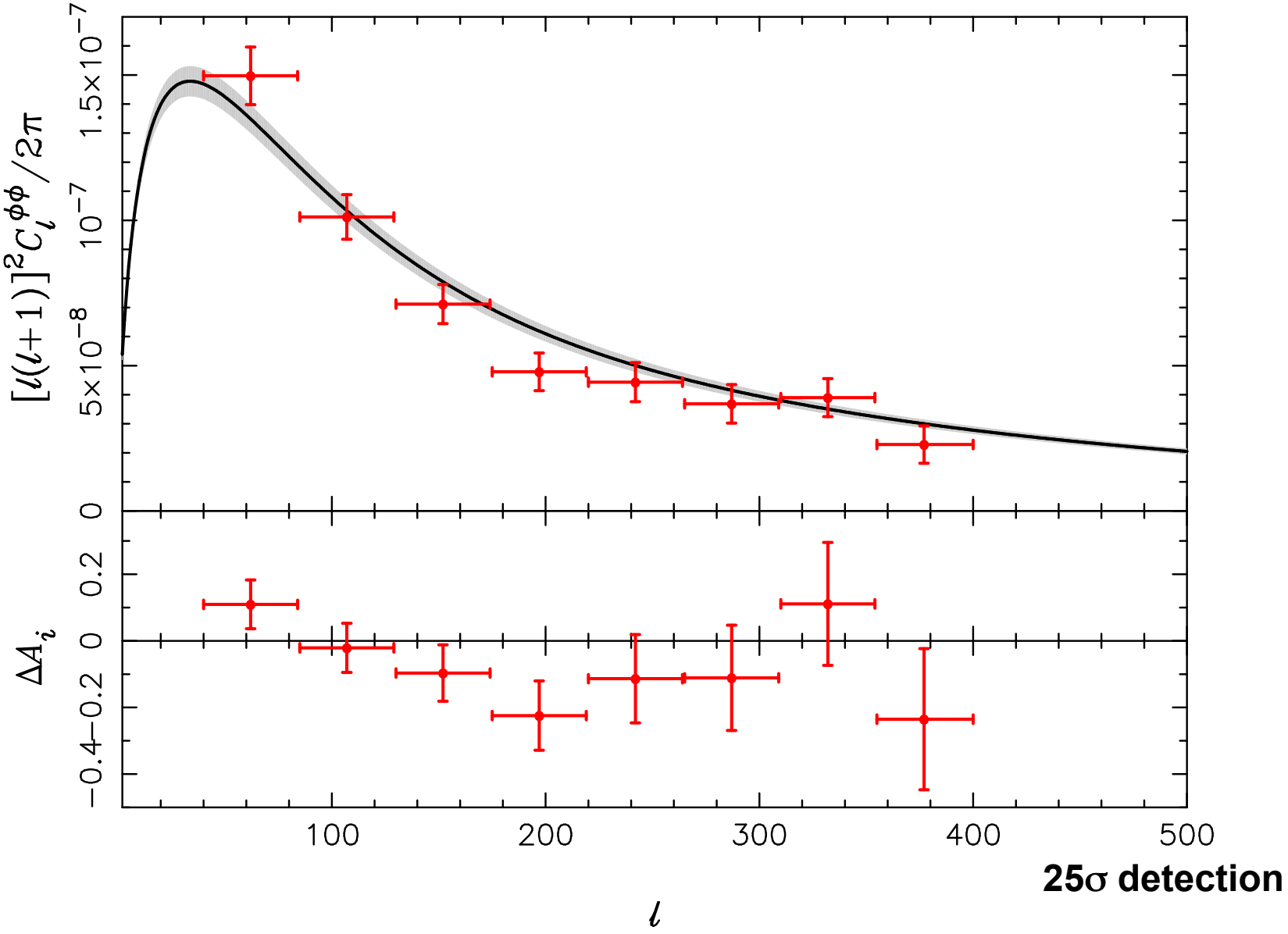

ΛCDM Cosmological Parameters

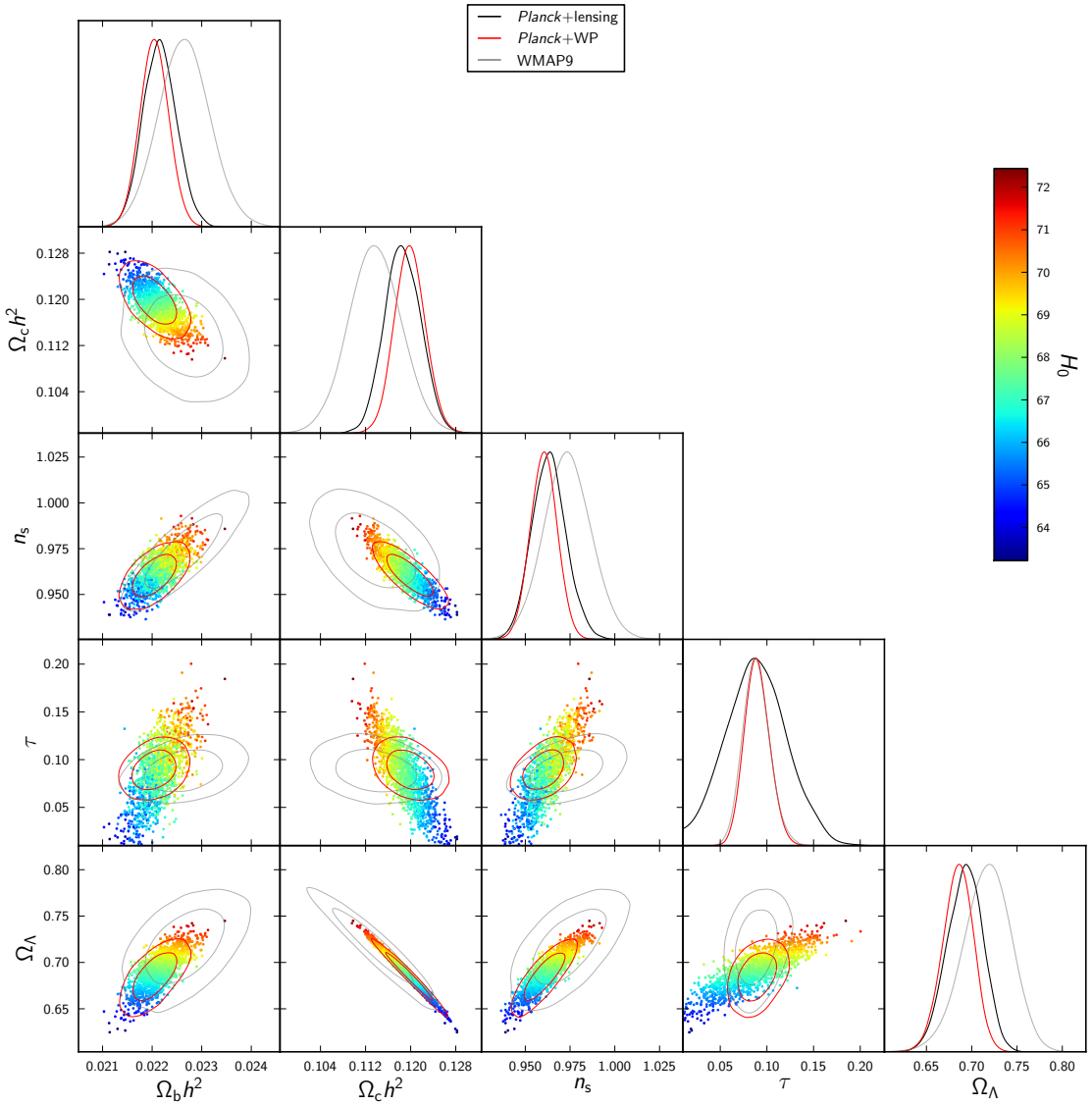

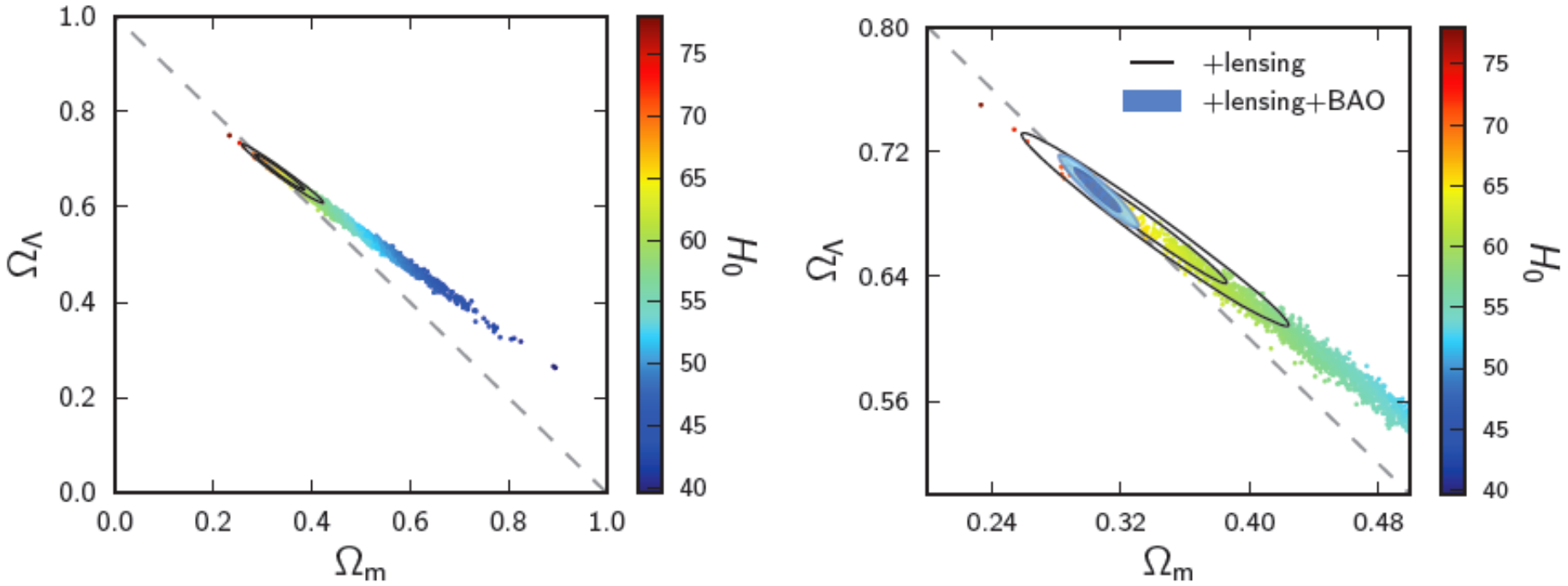

Fig. 25. The *Planck*+WP+highL data combination (samples; colour-coded by the value of H_0) partially breaks the geometric degeneracy between Ω_m and Ω_Λ due to the effect of lensing in the temperature power spectrum. These limits are significantly improved by the inclusion of the *Planck* lensing reconstruction (black contours). Combining also with BAO (right; solid blue contours) tightly constrains the geometry to be nearly flat.

Acoustic-scale distance ratio consistency between *Planck* and other experiments

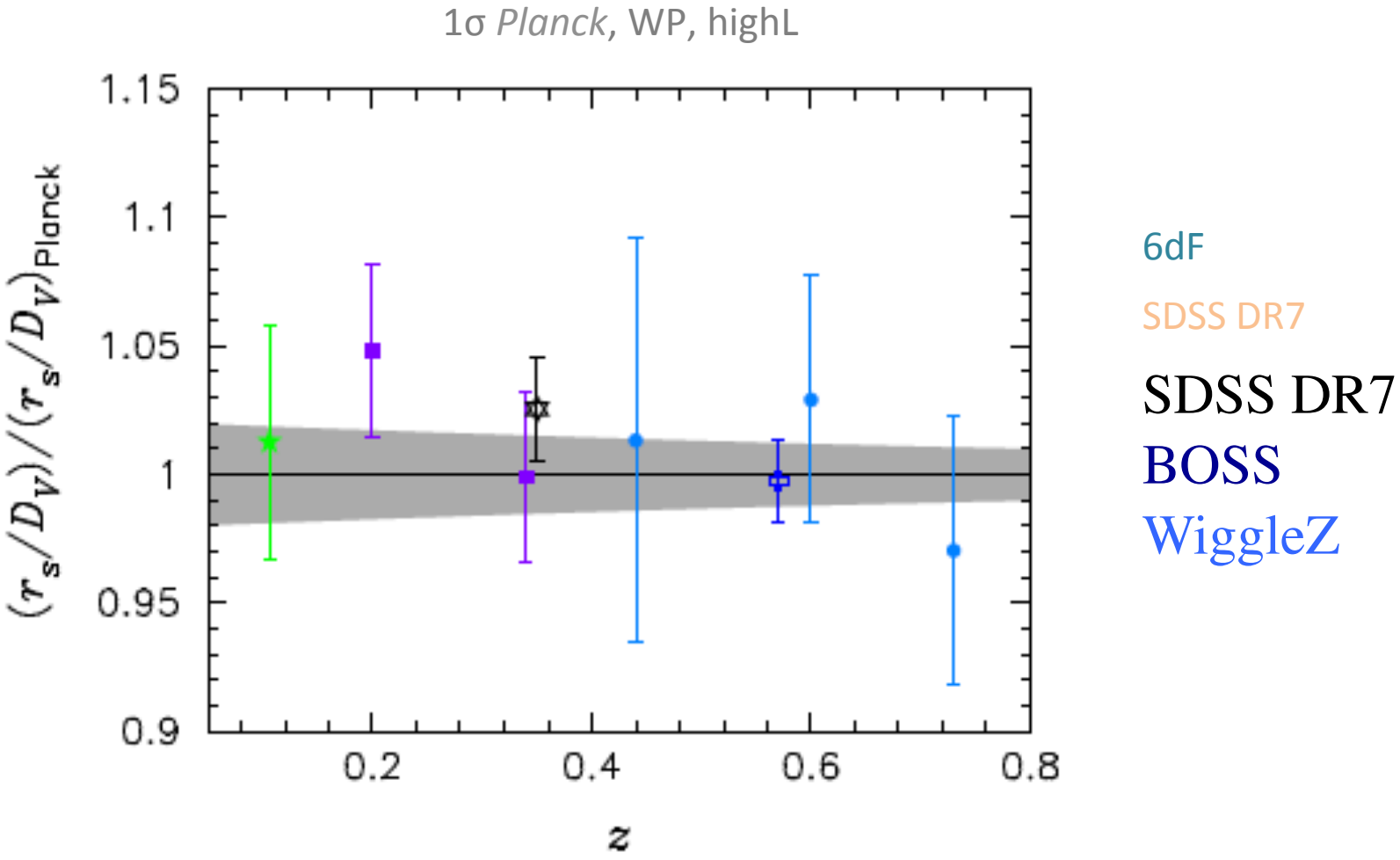

Acoustic-scale distance ratio consistency between WMAP, *Planck* and other experiments

WMAP 7 + SPT

1σ *Planck*, WP, highL

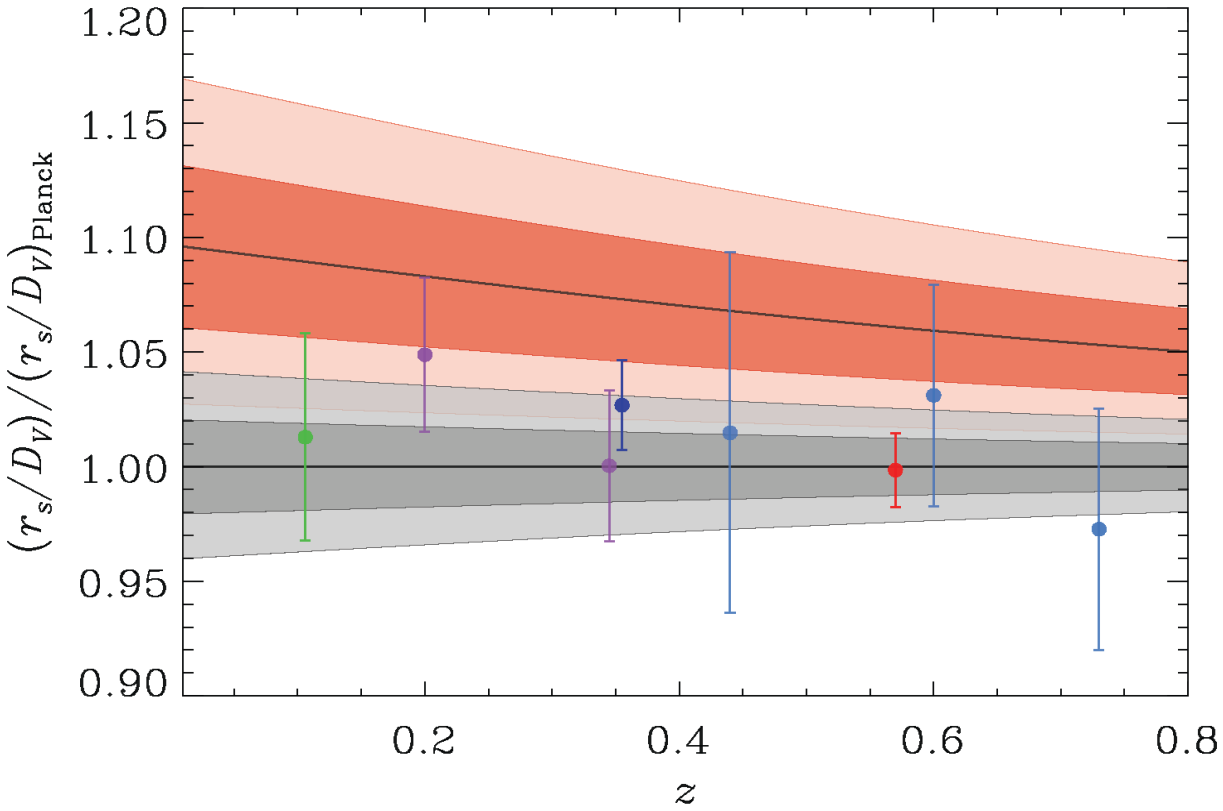

6dF

SDSS DR7

SDSS DR7

BOSS

WiggleZ

Consistency between *Planck* and BBN

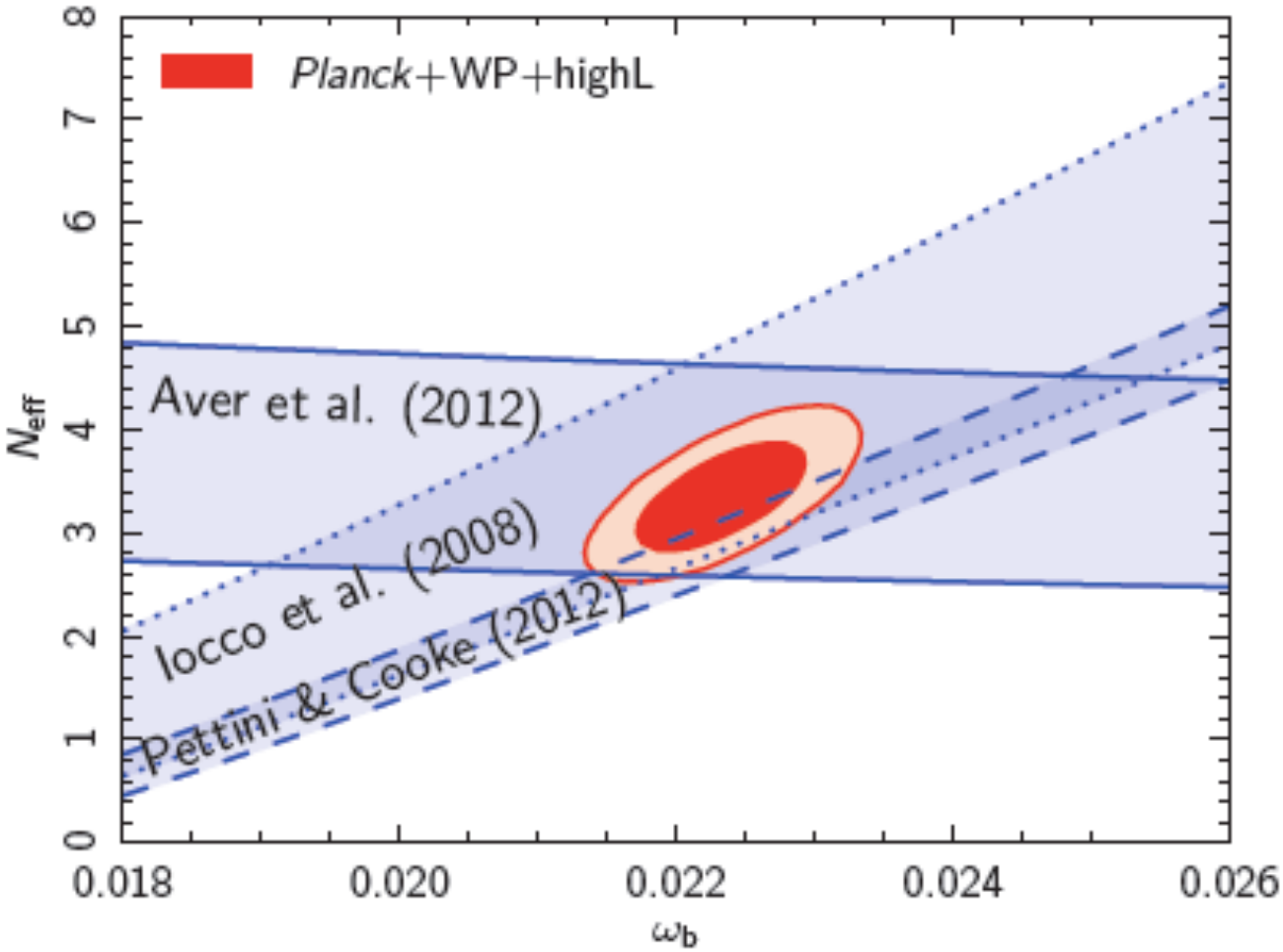

A determination of H_0 from the CMB alone

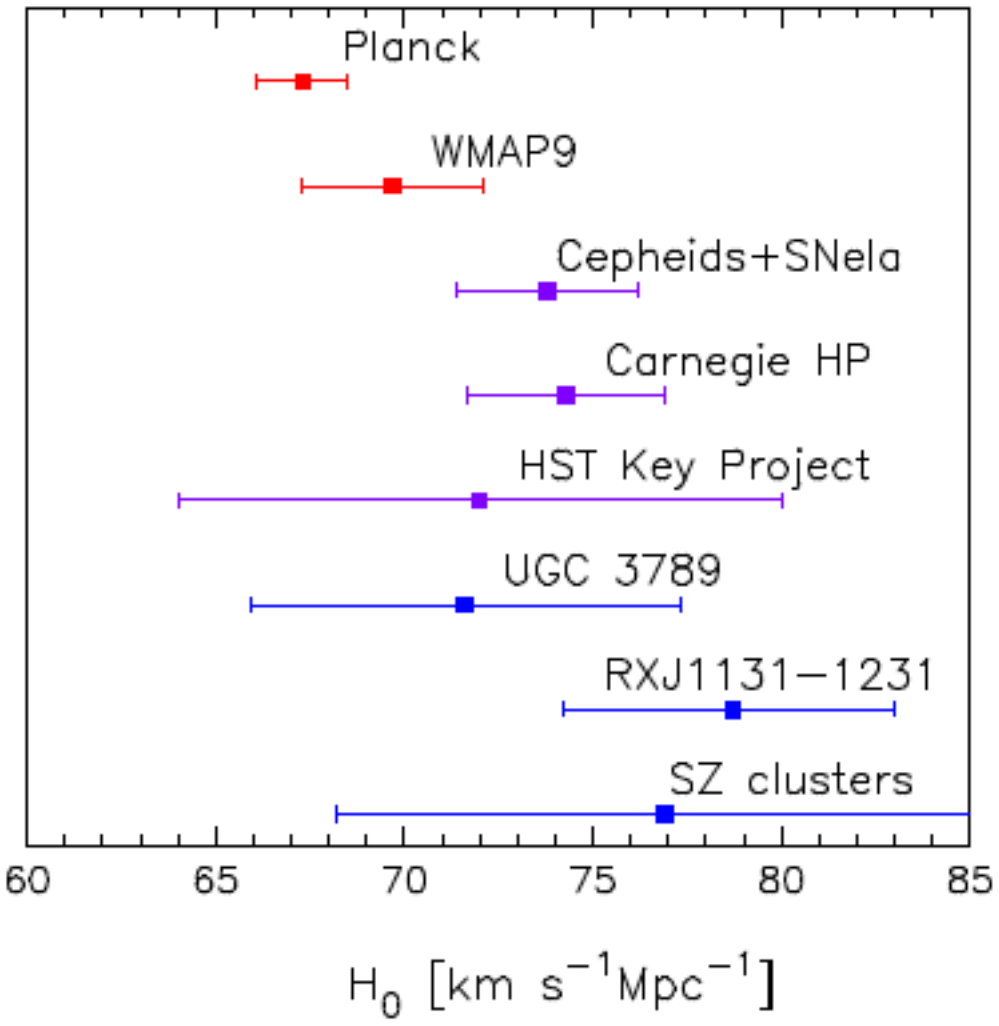

Ω_K
Σm_ν [eV]
$N_{\rm eff}$
$Y_{\rm P}$
$dn_{\rm s}/d\ln k$
$r_{0.002}$
w
$\Omega_b h^2$
$\Omega_c h^2$
$n_{\rm s}$
H_0
σ_8

Cosmological Summary:

- ΛCDM best fit driven by $80 < \ell < 2000$
- lensing breaks the geometric degeneracy (both lensed C_ℓ^{TT}, $C_\ell^{\varphi\varphi}$)
- ↑ baryons, ↑ dark matter, ↓ cosmological const.
- *excellent* agreement with BBN, BAO acoustic scale
- scale invariance ($n_s < 1$) ruled out at 5.4 sigma (CMB alone)
- low H_0 relative to HST
- no evidence for (data disfavor)
  - anything beyond the 3 standard neutrino species
  - curvature, running index, dynamical dark energy, isocurvature, sterile neutrinos, …
  - local type NG, $f_{NL} < 6$ or so.
- above multipole of 40, excellent agreement with ΛCDM
- below multipole of 40, the χ^2 doesn't tell the story…
- complicated disagreement with WMAP on the CMB

Table 9. Results for the f_{NL} parameters of the primordial local, equilateral, and orthogonal shapes, determined by the KSW, binned and modal estimators from the SMICA, NILC, SEVEM, and C-R foreground-cleaned maps. Both independent single-shape results and results marginalized over the point source bispectrum and with the ISW-lensing bias subtracted are reported; error bars are 68% CL.

	Independent			ISW-lensing subtracted		
	KSW	Binned	Modal	KSW	Binned	Modal
SMICA						
Local	9.8 ± 5.8	9.2 ± 5.9	8.3 ± 5.9	**2.7 ± 5.8**	2.2 ± 5.9	1.6 ± 6.0
Equilateral	−37 ± 75	−20 ± 73	−20 ± 77	**−42 ± 75**	−25 ± 73	−20 ± 77
Orthogonal	−46 ± 39	−39 ± 41	−36 ± 41	**−25 ± 39**	−17 ± 41	−14 ± 42
NILC						
Local	11.6 ± 5.8	10.5 ± 5.8	9.4 ± 5.9	4.5 ± 5.8	3.6 ± 5.8	2.7 ± 6.0
Equilateral	−41 ± 76	−31 ± 73	−20 ± 76	−48 ± 76	−38 ± 73	−20 ± 78
Orthogonal	−74 ± 40	−62 ± 41	−60 ± 40	−53 ± 40	−41 ± 41	−37 ± 43
SEVEM						
Local	10.5 ± 5.9	10.1 ± 6.2	9.4 ± 6.0	3.4 ± 5.9	3.2 ± 6.2	2.6 ± 6.0
Equilateral	−32 ± 76	−21 ± 73	−13 ± 77	−36 ± 76	−25 ± 73	−13 ± 78
Orthogonal	−34 ± 40	−30 ± 42	−24 ± 42	−14 ± 40	−9 ± 42	−2 ± 42
C-R						
Local	12.4 ± 6.0	11.3 ± 5.9	10.9 ± 5.9	6.4 ± 6.0	5.5 ± 5.9	5.1 ± 5.9
Equilateral	−60 ± 79	−52 ± 74	−33 ± 78	−62 ± 79	−55 ± 74	−32 ± 78
Orthogonal	−76 ± 42	−60 ± 42	−63 ± 42	−57 ± 42	−41 ± 42	−42 ± 42

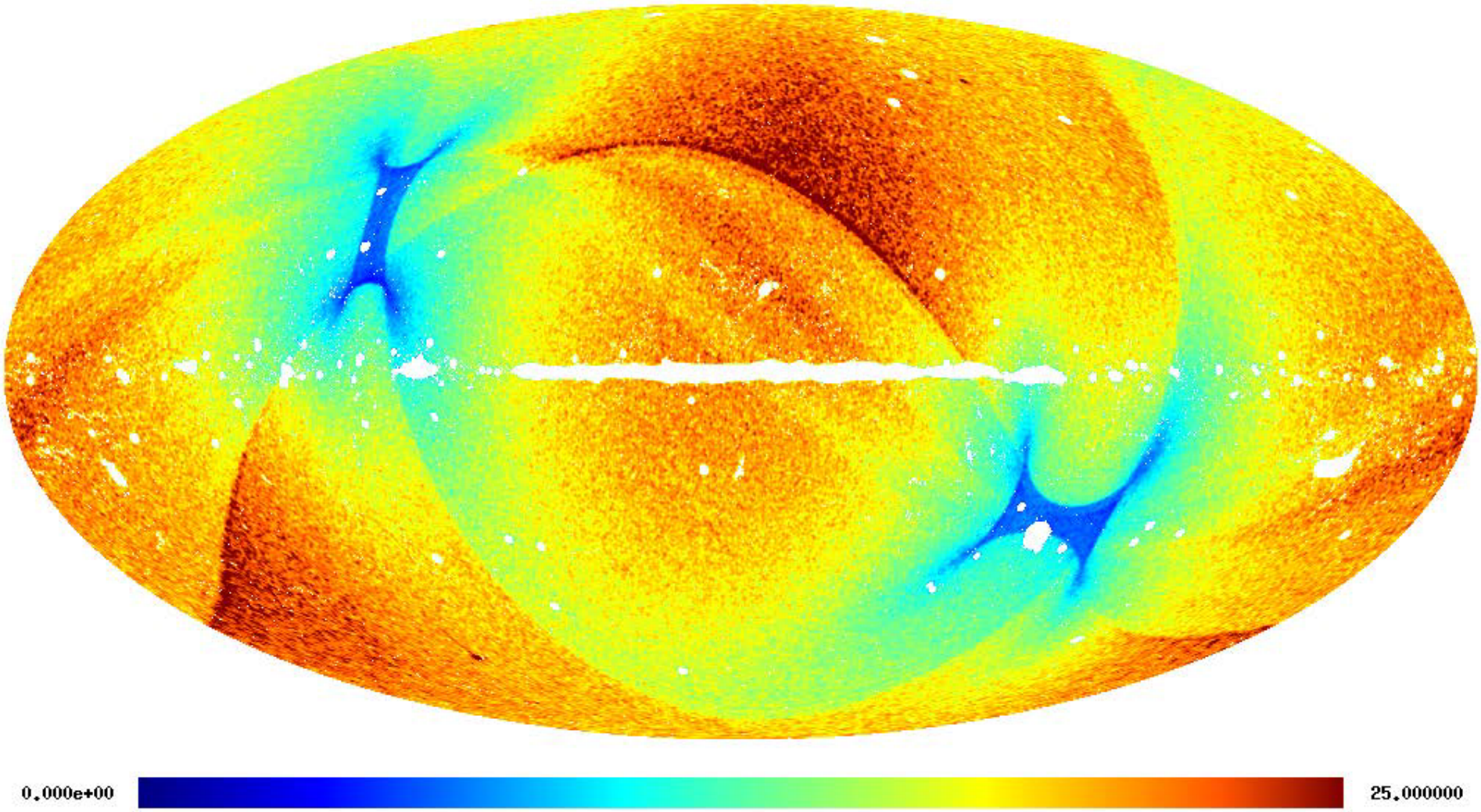
0.000e+00
25.000000

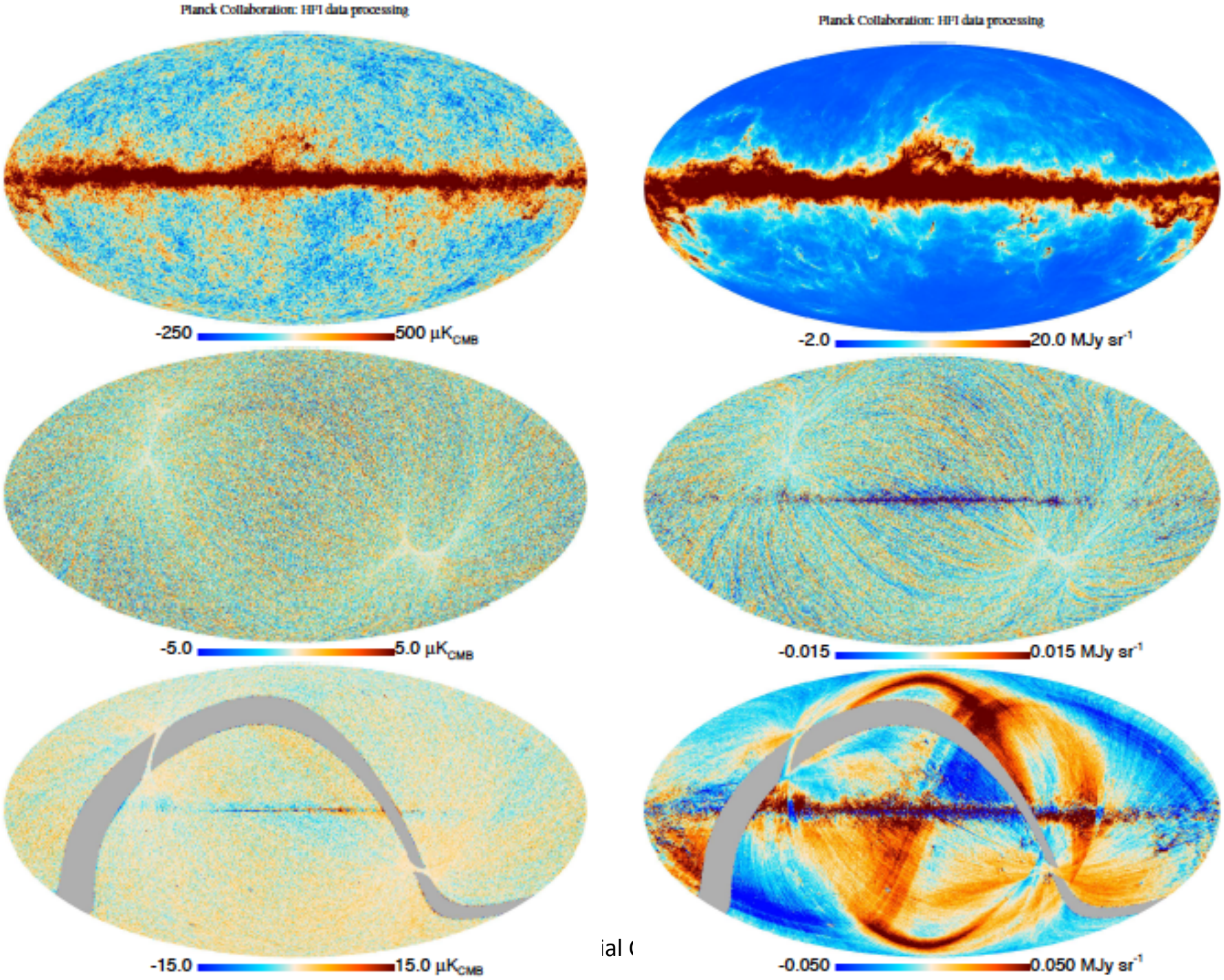
Planck Collaboration: HFI data processing
-250
500 μK$_{CMB}$
Planck Collaboration: HFI data processing
-2.0
20.0 MJy sr^{-1}
-5.0
5.0 μK$_{CMB}$
-0.015
0.015 MJy sr^{-1}
-15.0
15.0 μK$_{CMB}$
-0.050
0.050 MJy sr^{-1}

Table 19. Results for $f_{\rm NL}$ (assumed independent) of the SMICA half-ring null maps, determined by the KSW, binned and modal estimators.

SMICA half-ring	KSW	Binned	Modal
Local	-0.008 ± 0.18	-0.086 ± 0.20	-0.13 ± 0.35
Equilateral	-0.16 ± 2.2	1.3 ± 2.1	0.66 ± 2.0
Orthogonal	-0.035 ± 0.57	0.51 ± 0.57	0.14 ± 0.60
Diff ps - 1e29	-0.05 ± 0.60	0.03 ± 0.68	0.05 ± 0.65
ISW-lensing	$(-0.06 \pm 2.0) \times 10^{-3}$	$(-2.2 \pm 4.7) \times 10^{-3}$	0.009 ± 0.030

Table 20. Results for $f_{\rm NL}$ (assumed independent) of several null maps determined by the binned estimator. We consider half-ring $(r1 - r2)/2$, survey $(s2 - s1)/2$, and detector set $(d1 - d2)/2$ difference maps for SMICA and the raw 143 GHz channel.

Binned	SMICA half-ring	143 GHz half-ring	143 GHz survey	143 GHz detector set
Local	-0.086 ± 0.20	-0.016 ± 0.073	0.43 ± 0.56	1.9 ± 1.7
Equilateral	1.3 ± 2.1	3.2 ± 1.8	-1.5 ± 4.2	0.9 ± 5.8
Orthogonal	0.51 ± 0.57	1.2 ± 0.6	-1.7 ± 1.3	-1.3 ± 1.8
Diff ps - 1e29	0.03 ± 0.68	0.19 ± 1.9	3.4 ± 3.2	-1.0 ± 4.3
ISW-lensing	$(-2.2 \pm 4.7) \times 10^{-3}$	$(-0.5 \pm 1.7) \times 10^{-3}$	$(-0.6 \pm 11) \times 10^{-3}$	0.033 ± 0.026

Table 21. Summary of our $f_{\rm NL}$ analysis of foreground residuals. For realistic lensed FFP6 simulations processed through the SMICA and NILC component separation pipelines, we report: the average $f_{\rm NL}$ with and without foreground residuals added to the maps, the $f_{\rm NL}$ standard deviation in the same two cases, and the standard deviation of the map-by-map $f_{\rm NL}$ difference between the "clean" and "contaminated" sample. The impact of foreground residuals is clearly subdominant when compared to statistical error bars for all shapes. Results reported below have been obtained using the modal estimator.

Modal	SMICA clean	SMICA residual	NILC clean	NILC residual	SMICA residual – clean	NILC residual – clean
Local	7.7 ± 5.9	7.8 ± 5.9	7.7 ± 5.8	7.4 ± 6.0	0.04 ± 1.0	-0.27 ± 1.1
Equilateral	-0.5 ± 77	-8.7 ± 79	-0.6 ± 78	-9.0 ± 79	-8.3 ± 8.2	-8.4 ± 8.3
Orthogonal	-23 ± 41	-25 ± 41	-24 ± 40	-26 ± 41	-2.0 ± 4.7	-2.4 ± 4.8
ISW-lensing	1.00 ± 0.38	1.01 ± 0.38	1.01 ± 0.38	1.02 ± 0.38	0.006 ± 0.052	0.013 ± 0.052

Constraints on Inflation: n_s is robust

Two key results:

robust detection of a blue tilt: $n_s = 0.9585 \pm 0.0070$

a "low" value of the Hubble constant: $H_0 = 67.3 \pm 1.2$ km/s/Mpc

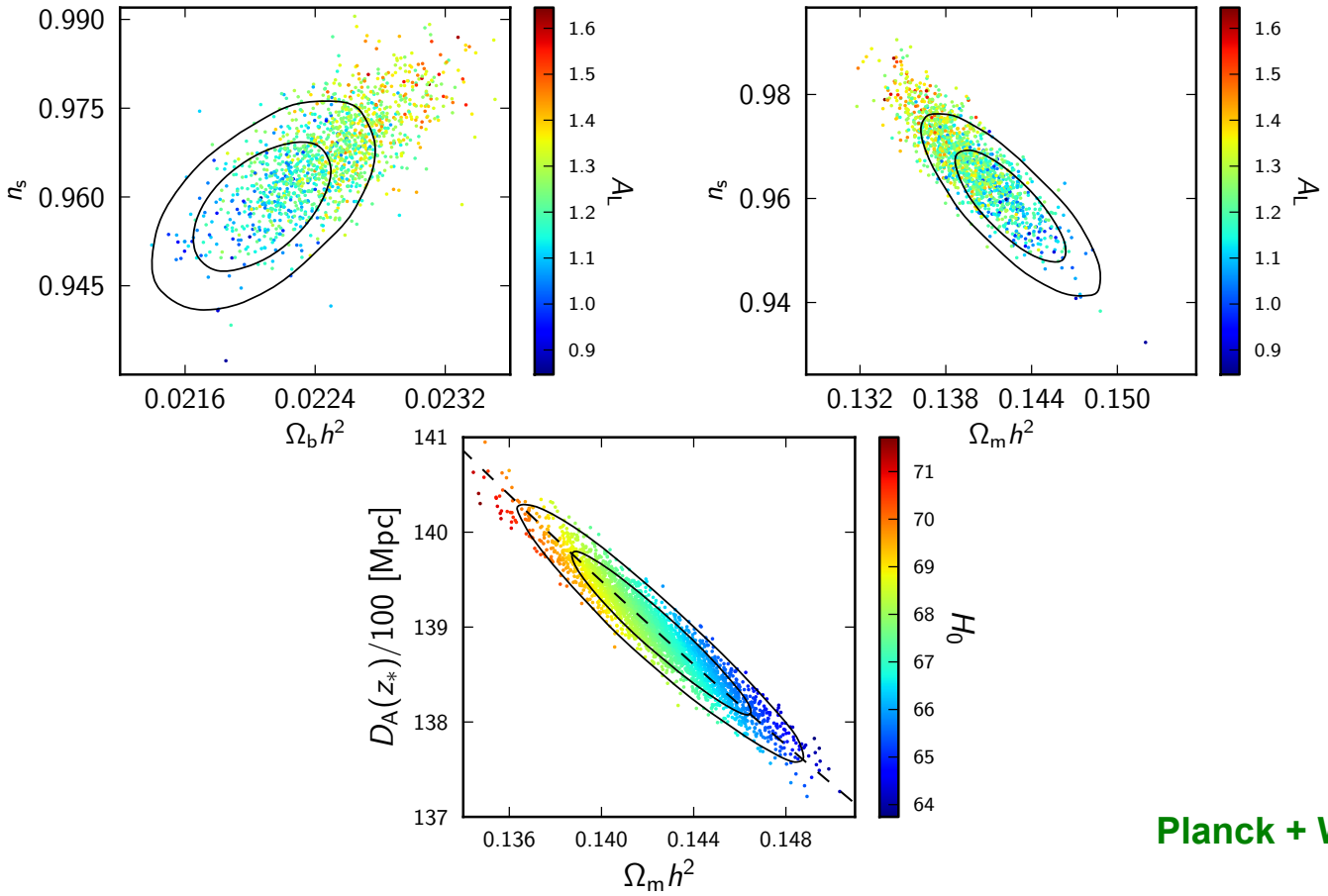

Planck + WP + highL

Constraints on Inflation

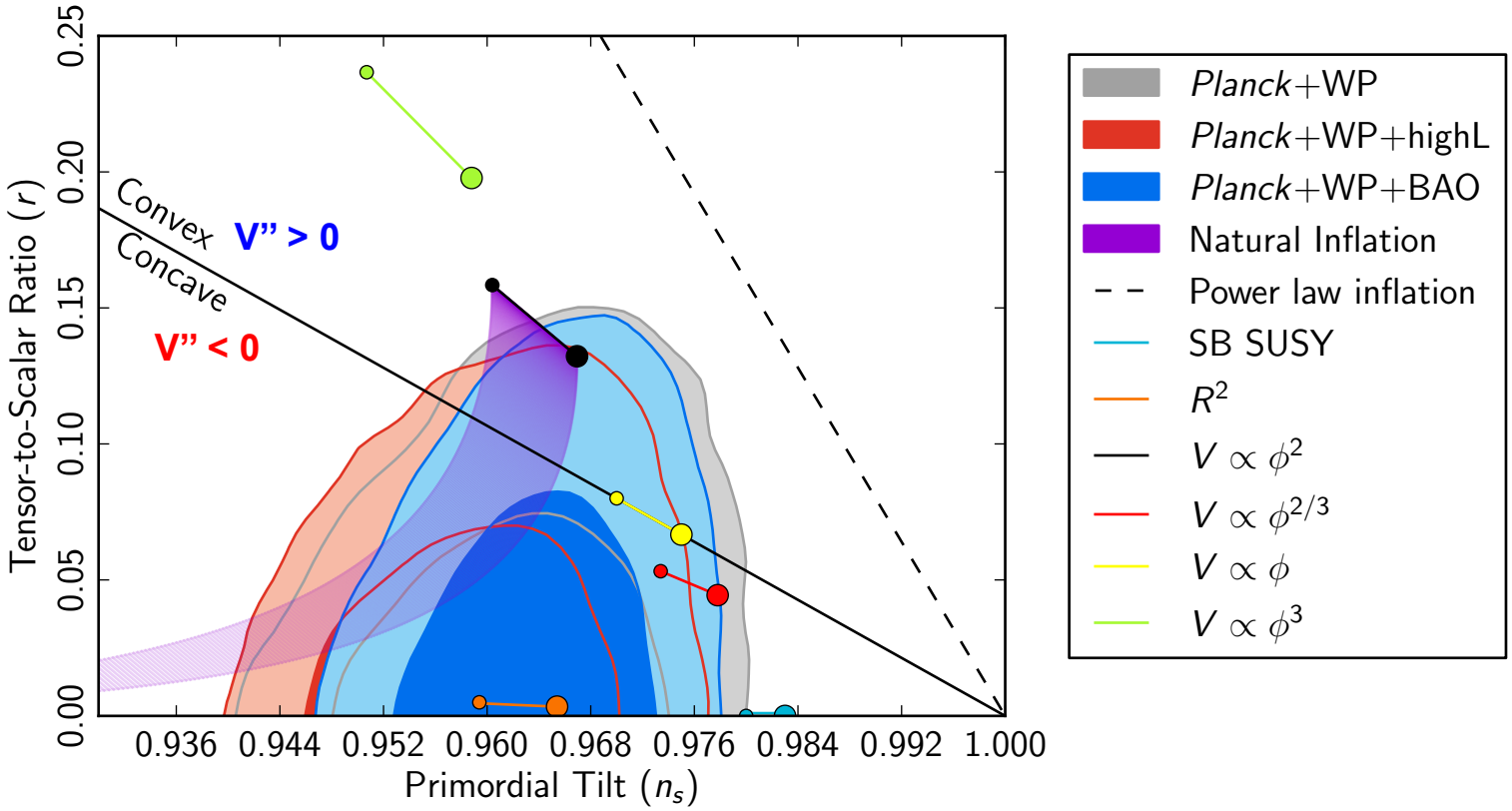

PHYSICAL REVIEW D 82, 043003 (2010)

Relic gravitational waves in light of the 7-year Wilkinson Microwave Anisotropy Probe data and improved prospects for the Planck mission

W. Zhao,[1,2,3,*] D. Baskaran,[1,2,†] and L. P. Grishchuk[1,4,‡]

VI. THEORETICAL FRAMEWORKS THAT WILL BE ACCEPTED OR REJECTED BY PLANCK OBSERVATIONS

Our forecast for the Planck mission, as any forecast in nature, can prove its value only after actual observation. We predict sunny days of confident detection of relic gravitational waves, but the reality can turn out to be gloomy days of continuing uncertainty. One can illustrate this point with the help of probability distributions in

Polnarev, et al.

Mon. Not. R. Astron. Soc. **386,** 1053–1063 (2008)

$$(\mathrm{S/N})_{\mathrm{TE}} = \sqrt{2}\gamma \frac{r}{\alpha + \beta r} \approx \sqrt{2}\gamma \frac{r}{\alpha}.$$

Status of CMB Polarization Observations

Balloon:
Boomerang
Maxipol
Ebex
Spider
Piper

Ground:
DASI
CBI
QUAD
Bicep1/2
CAPMAP
QUIET
Keck Array
ABS
PolarBear
CLASS

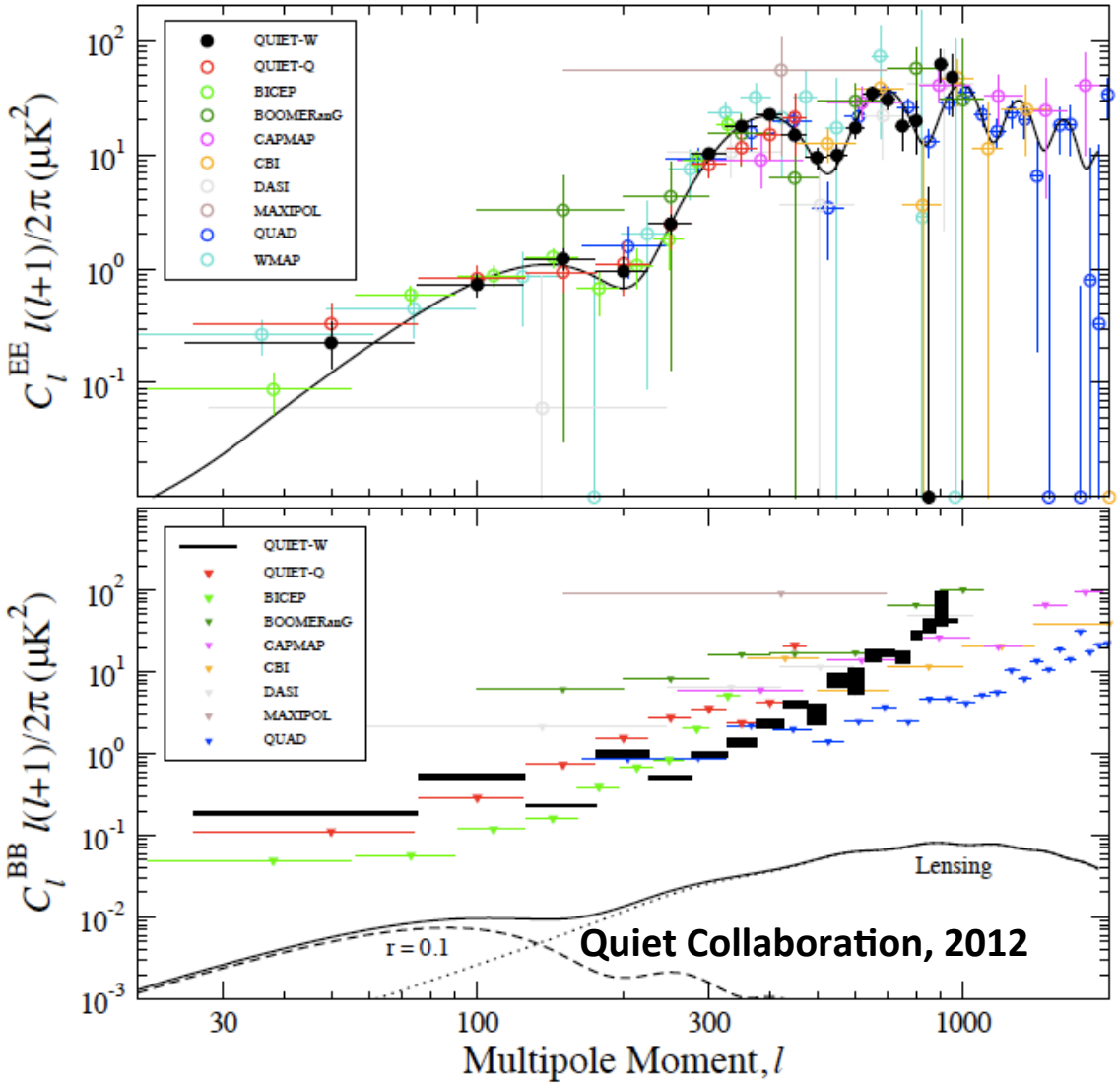

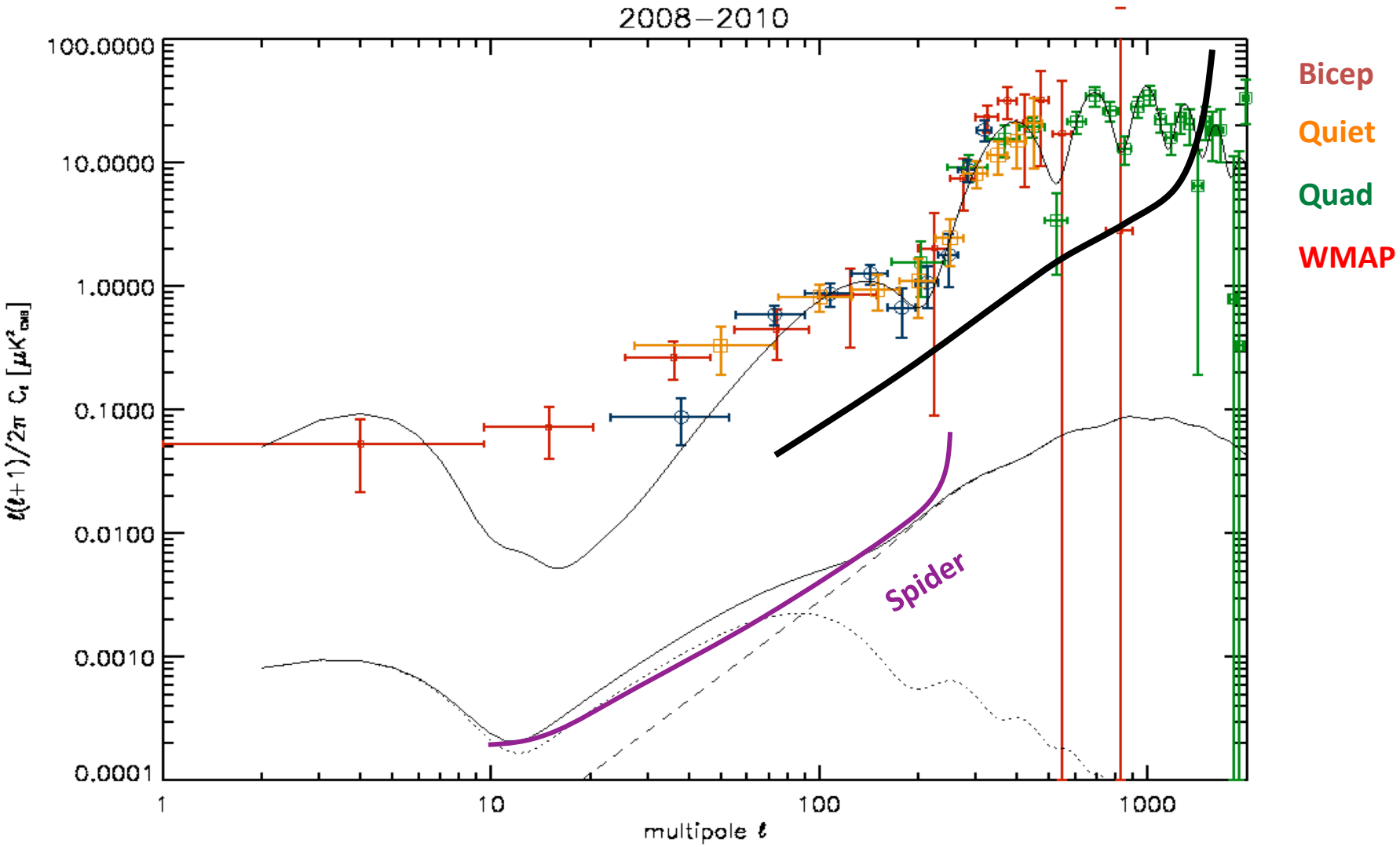
2008–2010
100.0000
10.0000
1.0000
0.1000
0.0100
0.0010
0.0001
1
10
100
1000
multipole ℓ
ℓ(ℓ+1)/2π Cℓ [μK²CMB]
Bicep
Quiet
Quad
WMAP
Spider

SPIDER

Suborbital Polarimeter for Inflation Dust and the Epoch of Reionization

- Long duration (20+ day cryogenic hold time) balloon borne polarimeter
- Sensitive to scales from 20° to 0.5°
- Instrumental sensitivities 5x that of Planck
- Polarization modulation and survey redundancy
- Technical Pathfinder: solutions appropriate for a space mission

NASA NSF CSA ASC C.S.B.F. PALESTINE, TEXAS NSERC CRSNG JPL NIST the David & Lucile Packard FOUNDATION CASE WESTERN RESERVE UNIVERSITY EST. 1826 UNIVERSITY OF TORONTO CARDIFF UNIVERSITY PRIFYSGOL CAERDYDD UBC PRINCETON UNIVERSITY UNIVERSITY OF KWAZULU-NATAL INYUVESI YAKWAZULU-NATALI CITA ICAT Canadian Institute for Theoretical Astrophysics L'Institut canadien d'astrophysique theorique Imperial College London

SPIDER

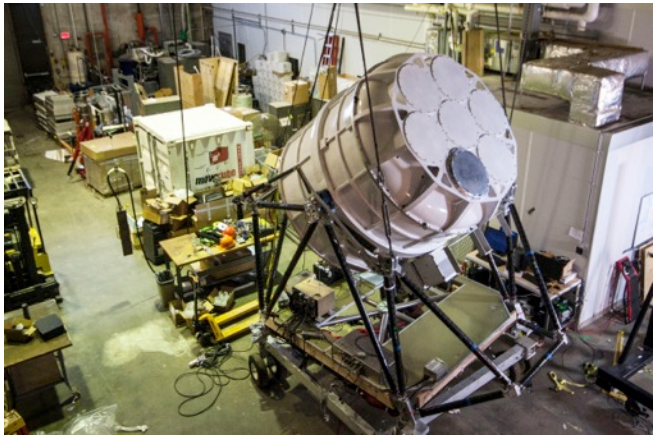

- 94/150 GHz flight in 2013/14 (~2600 detectors)
- 8% full sky, 0.27/0.20 $\mu K_{CMB}/deg^2$
- 5x Planck's sensitivity
- Probing Inflation at r ~ 0.03
- Detect weak lensing
- Detect Galactic polarization

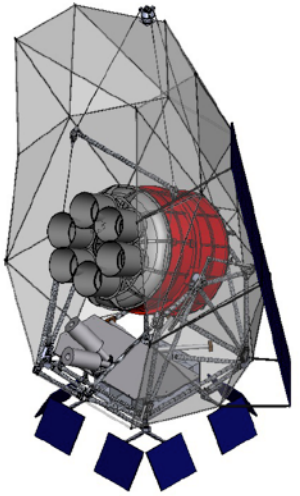

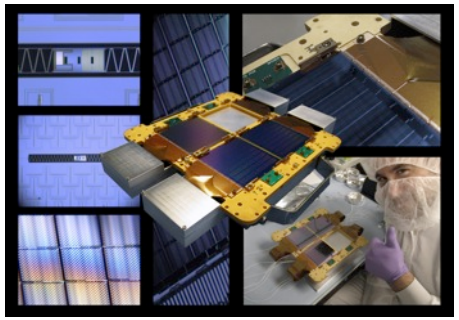

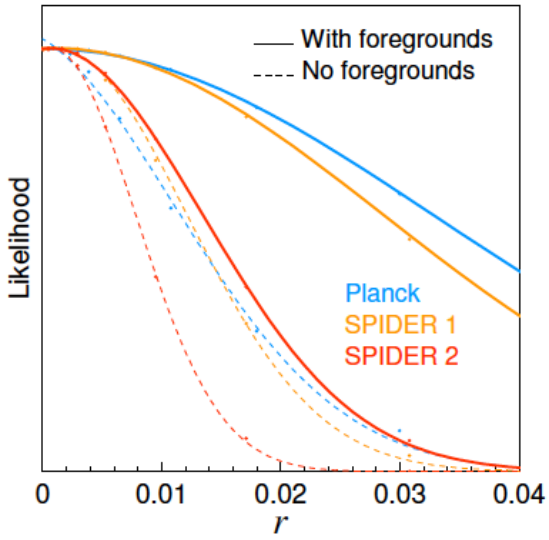

CMB Polarization Power Spectra: Polarization

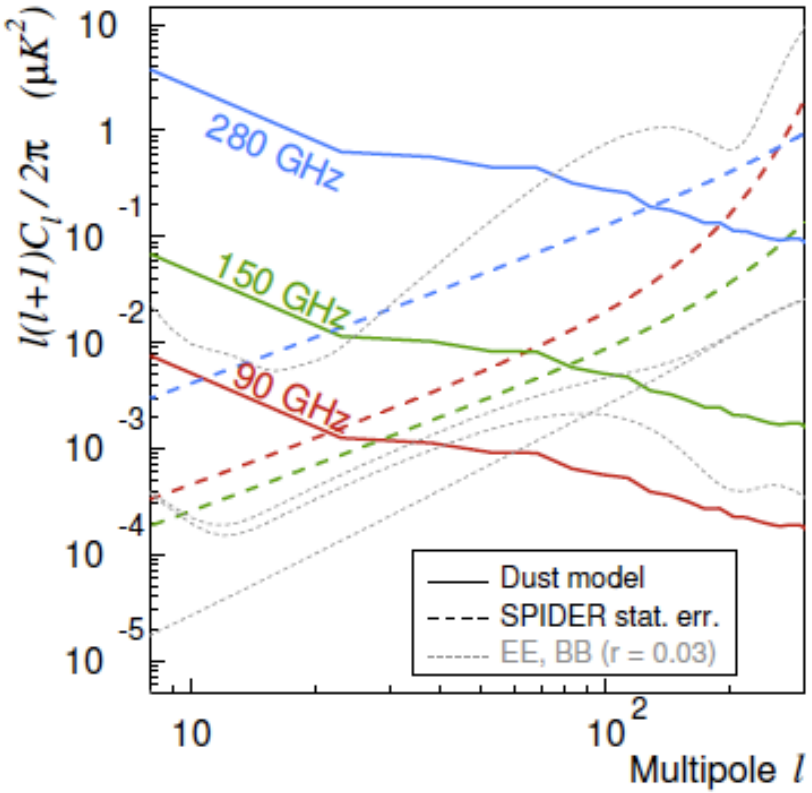

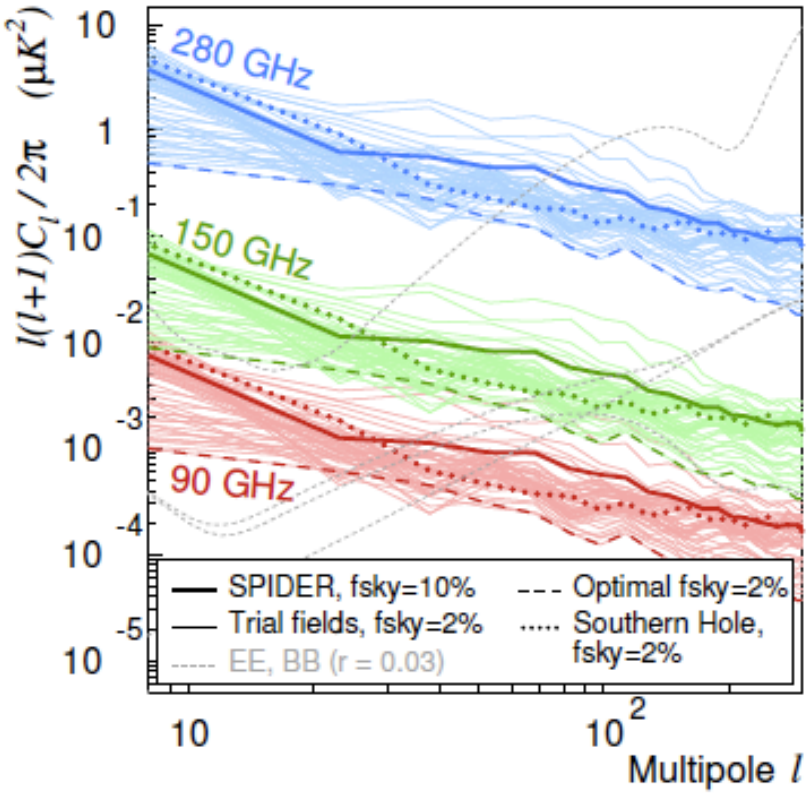

Fraisse, et al (2011)

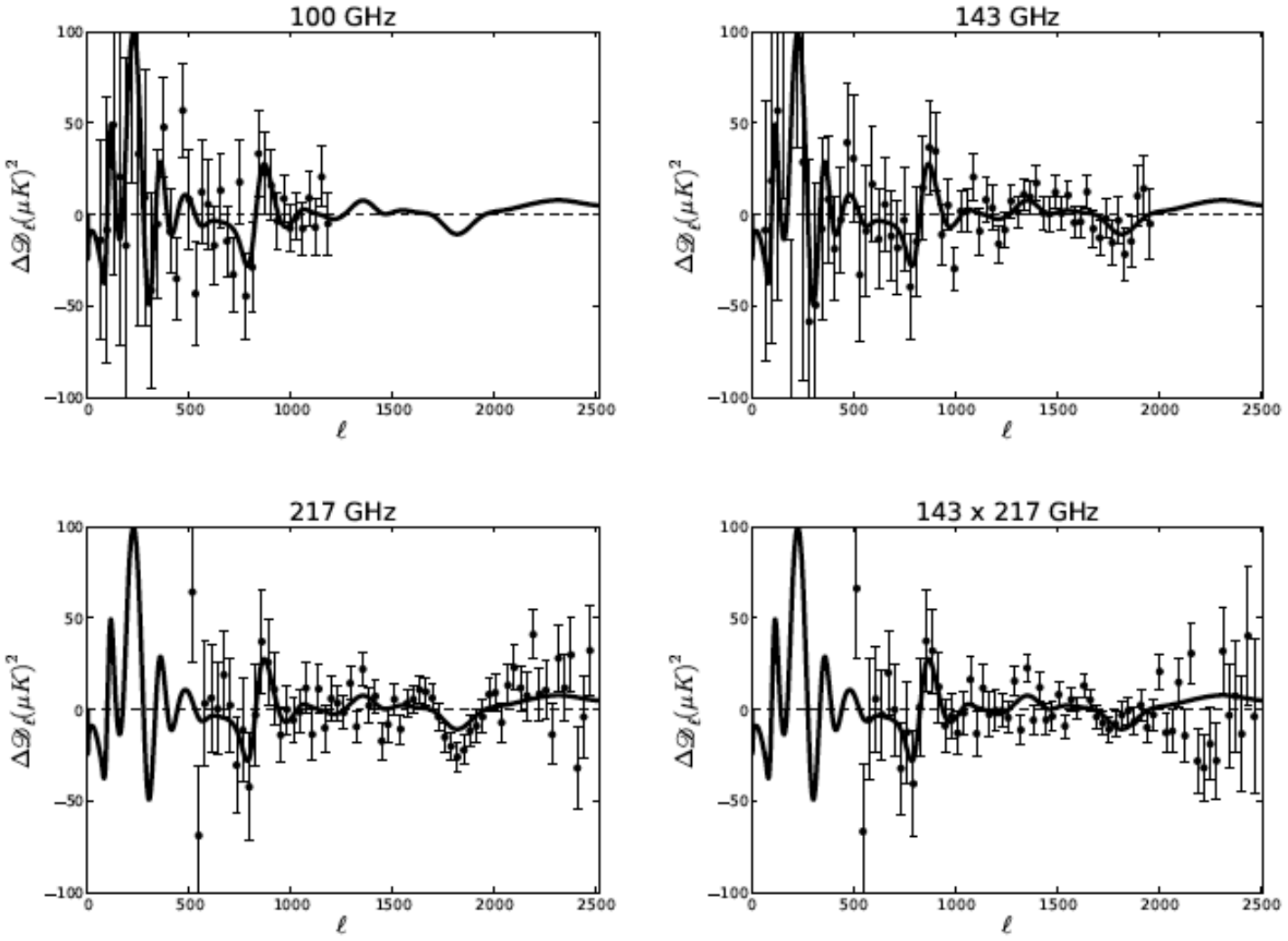

Fig. 16. CMB multipole spectrum residuals for best fit primordial power spectrum reconstruction at $\lambda = 10^3$. The panels show the C_ℓ spectrum residuals (compared to the best fit power law fiducial model represented by the horizontal straight dashed line) for the four auto- and cross-spectra included in the high-ℓ likelihood. Here, $D_\ell = (\ell(\ell+1)/(2\pi))C_\ell$. The data points have been binned with $\Delta\ell = 31$ and foregrounds subtracted according to the best fit foreground parameters. The solid black line shows the CMB spectrum residual for the maximum likelihood primordial power spectrum reconstruction with smoothing parameter $\lambda = 10^3$.

Would the real Planck please stand up?

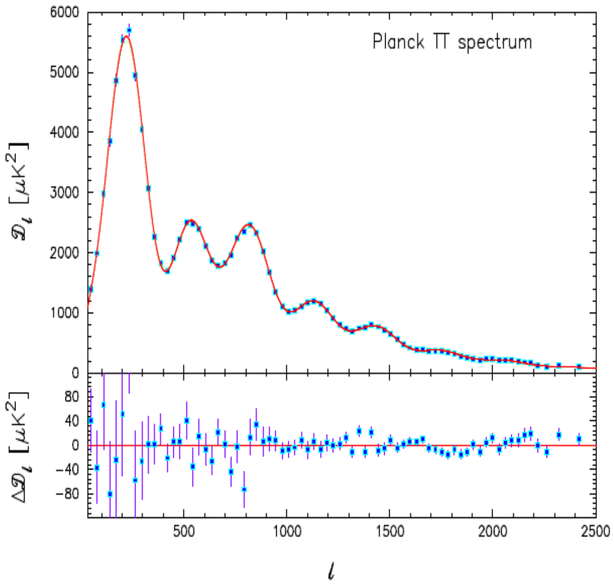

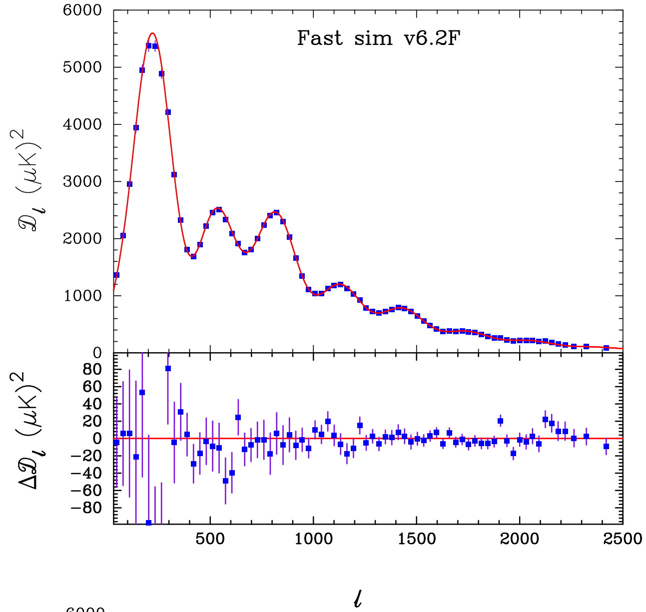

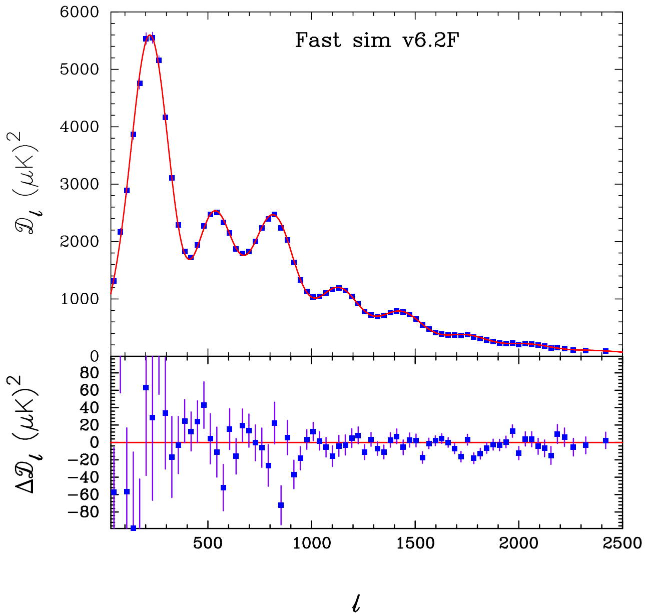

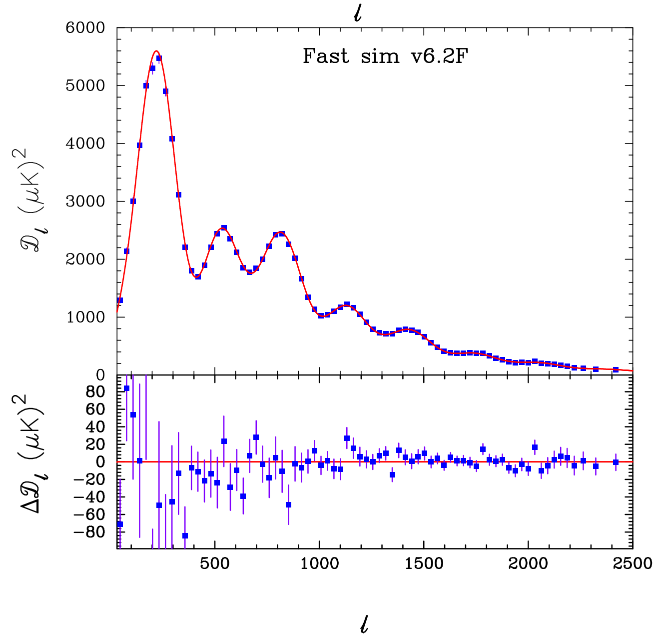

Survey null tests fail with high significance (and low amplitude)

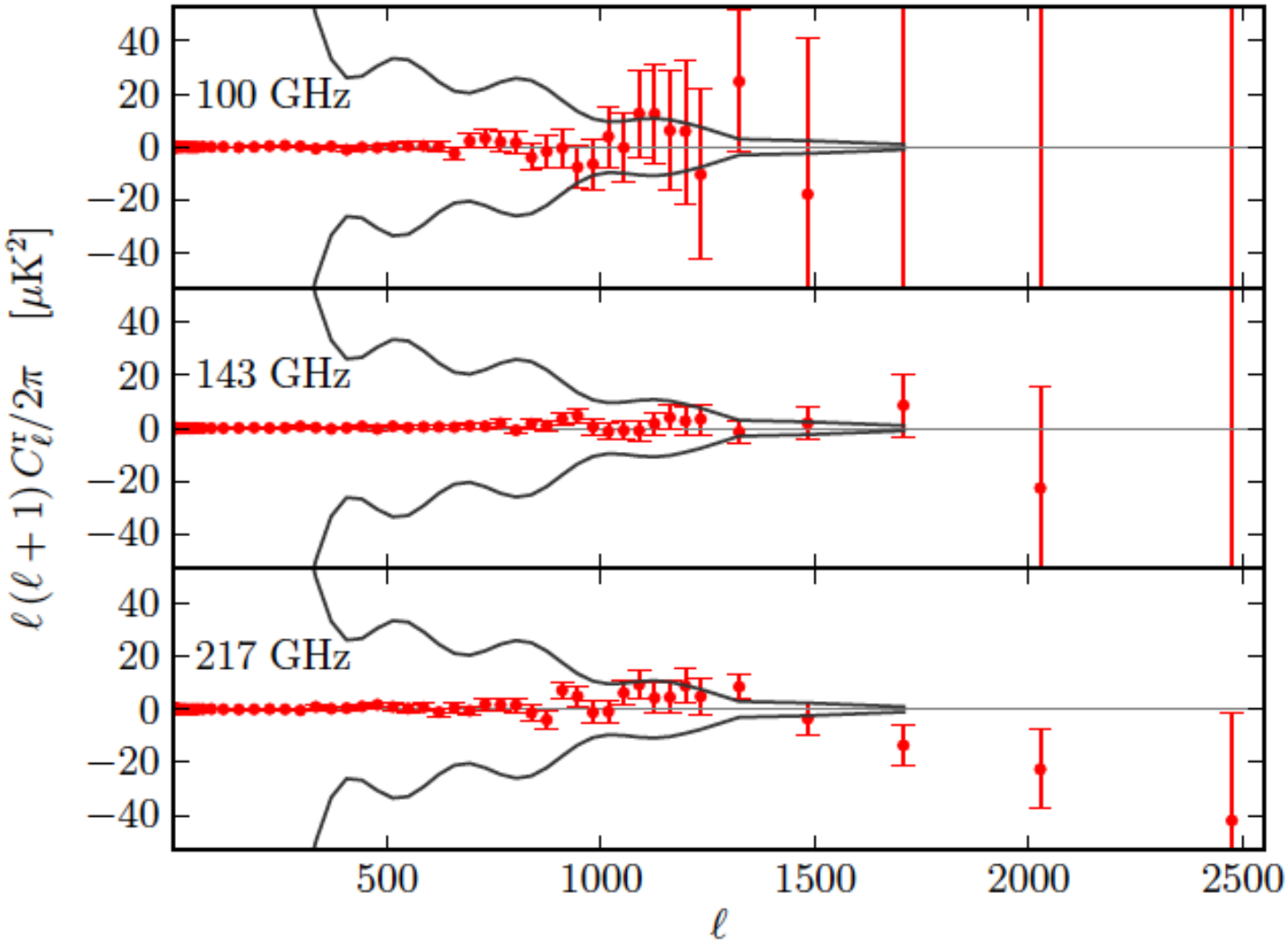

CMB Power Spectrum on the Larger Scales

The high-ℓ *Planck* data essentially determine the best-fit ΛCDM model.
This model gives more large-scale power than can be seen in the data.

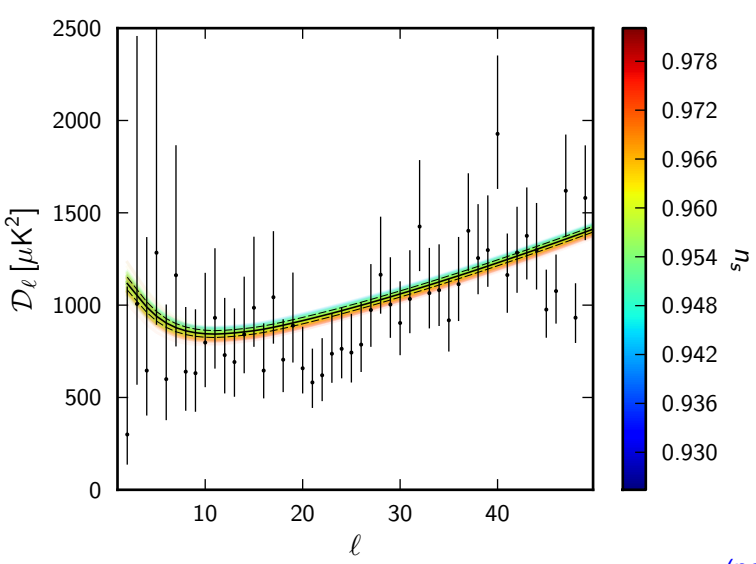

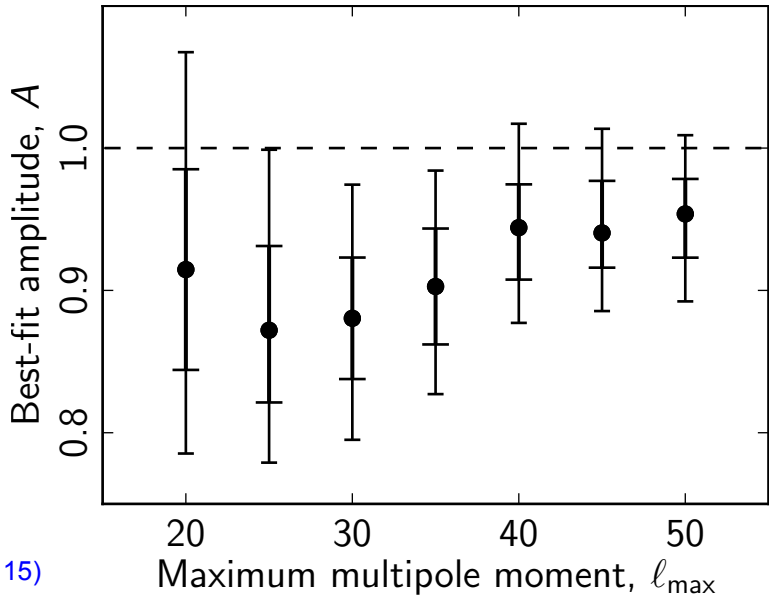

(paper 15)

This effect requires the whole range of multipoles measured by *Planck* to be seen.

All the "anomalies" previously detected by *WMAP* are still detected, now with higher statistical significance, by *Planck* (paper 23).

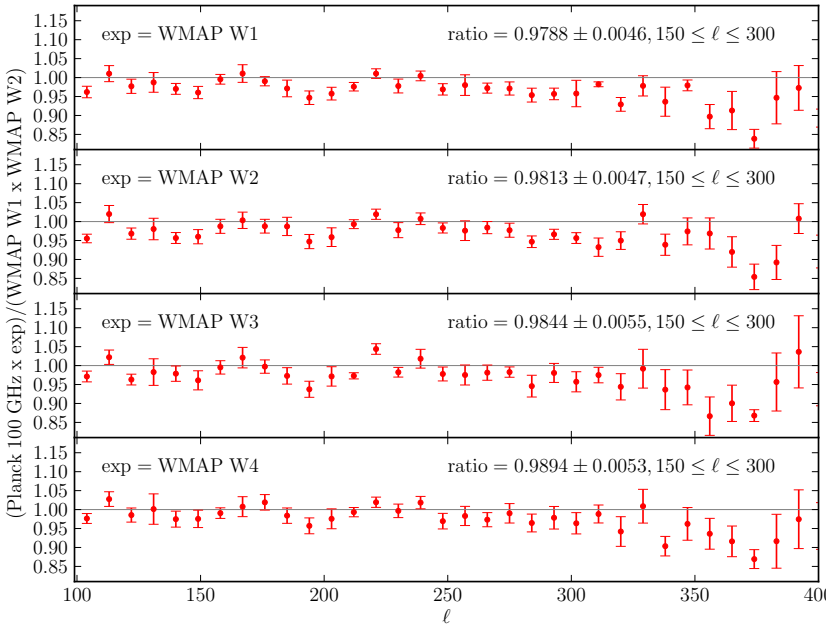

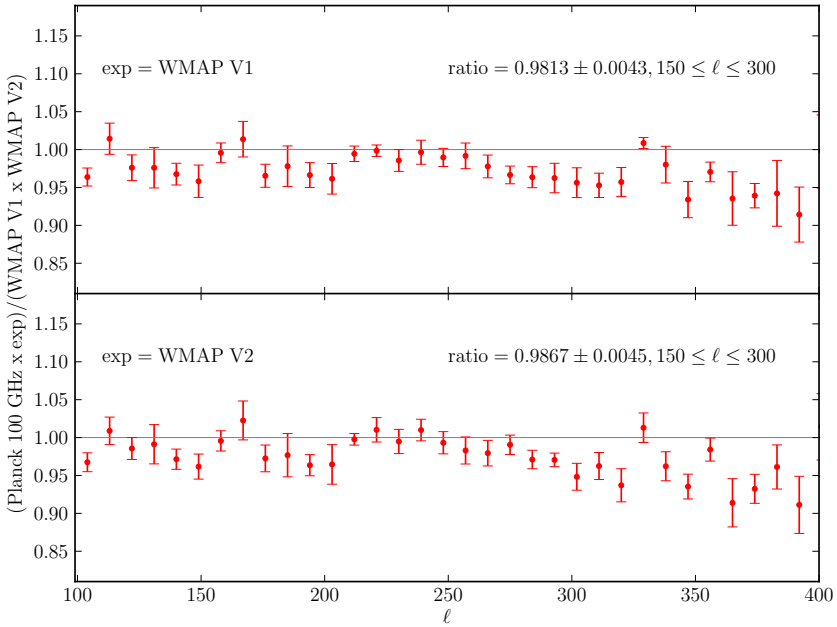

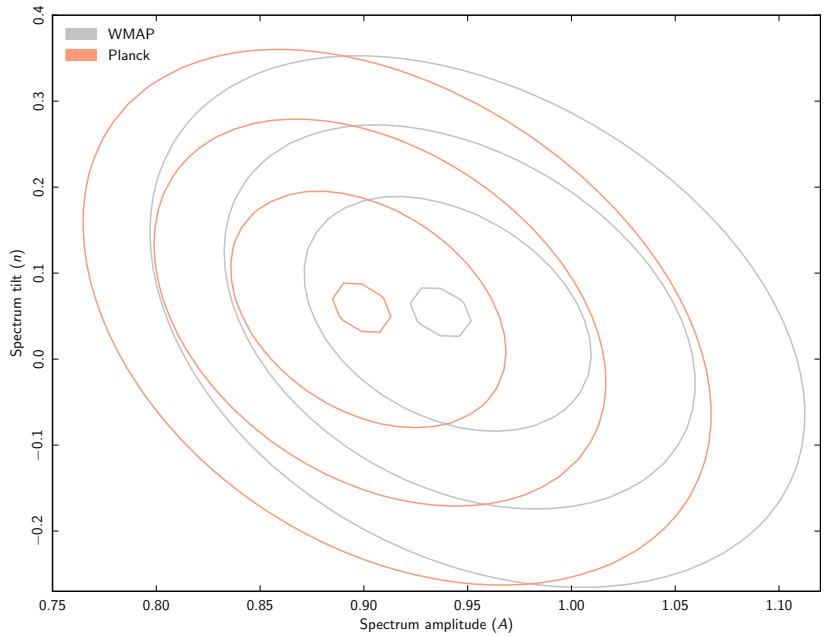

exp	Ratio mean	Ratio sigma	Side of WMAP focal plane
WMAP W1	1.0097	0.0015	Left
WMAP W2	1.0120	0.0017	Left
WMAP W3	1.0149	0.0016	Right
WMAP W4	1.0186	0.0015	Right
WMAP V1	1.0082	0.0035	Left
WMAP V2	1.0133	0.0034	Right
LFI 70 GHz	1.0002	0.0023	N/A

WMAP / Planck

Planck sees less power than *WMAP* at large angular scales.

As they stand, our and *WMAP's* error budgets cannot explain a difference at this level.

Band [GHz]	Solid Angle [arcmin^2]	Time Response	Near Sidelobes	Colour Correction	Monte Carlo
100	104.2	-0.030 ± 0.04 %	0.10 (0.18)%	< 0.3%	0.53%
143	58.4	-0.027 ± 0.013 %	0.15 (0.18)%	< 0.3%	0.14%
217	26.9	-0.025 ± 0.01 %	0.14 (0.17)%	< 0.3%	0.11%
353	25.1	-0.002 ± 0.0013 %	0.20 (0.24)%	< 0.5%	0.10%
545	25.4	0.035 ± 0.001 %	0.11 (0.18)%	< 2.0%	0.13%
857	23.0	0.092 ± 0.0006 %	0.23 (0.24)%	< 1.0%	0.15%

***Planck* beam error budget**

The absolute calibration of the *Planck* CMB channels is known to better than 0.4%.

The overall uncertainty at these scales in the *Planck* data is smaller than 1%.

WMAP / Planck

Planck sees less power than *WMAP* at large angular scales.

As they stand, our and WMAP's error budgets cannot explain a difference at this level.

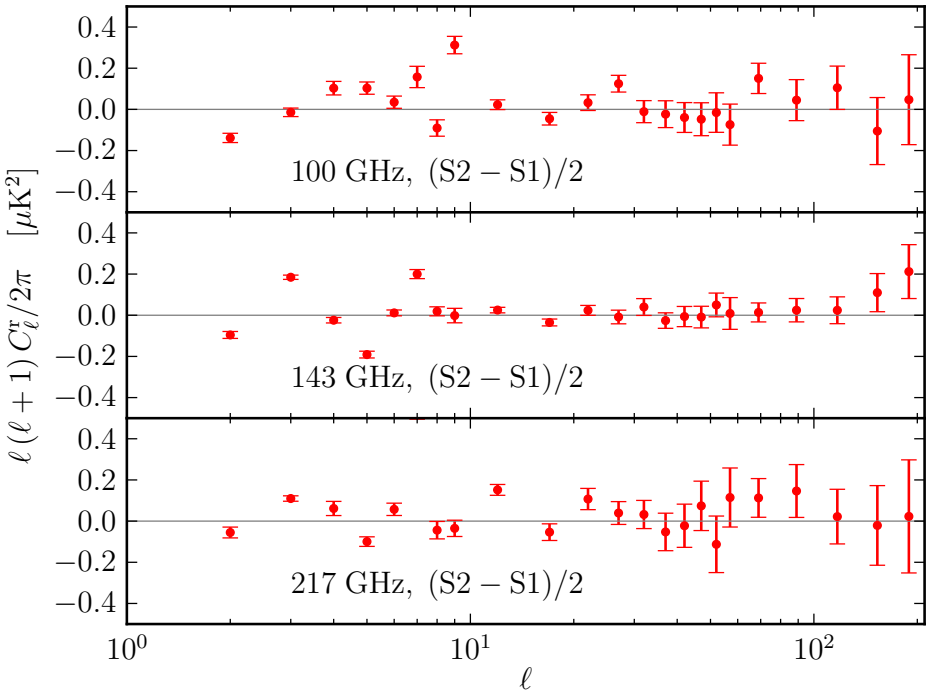

We do not see evidence in the *Planck* data of residual systematic errors at large scales.

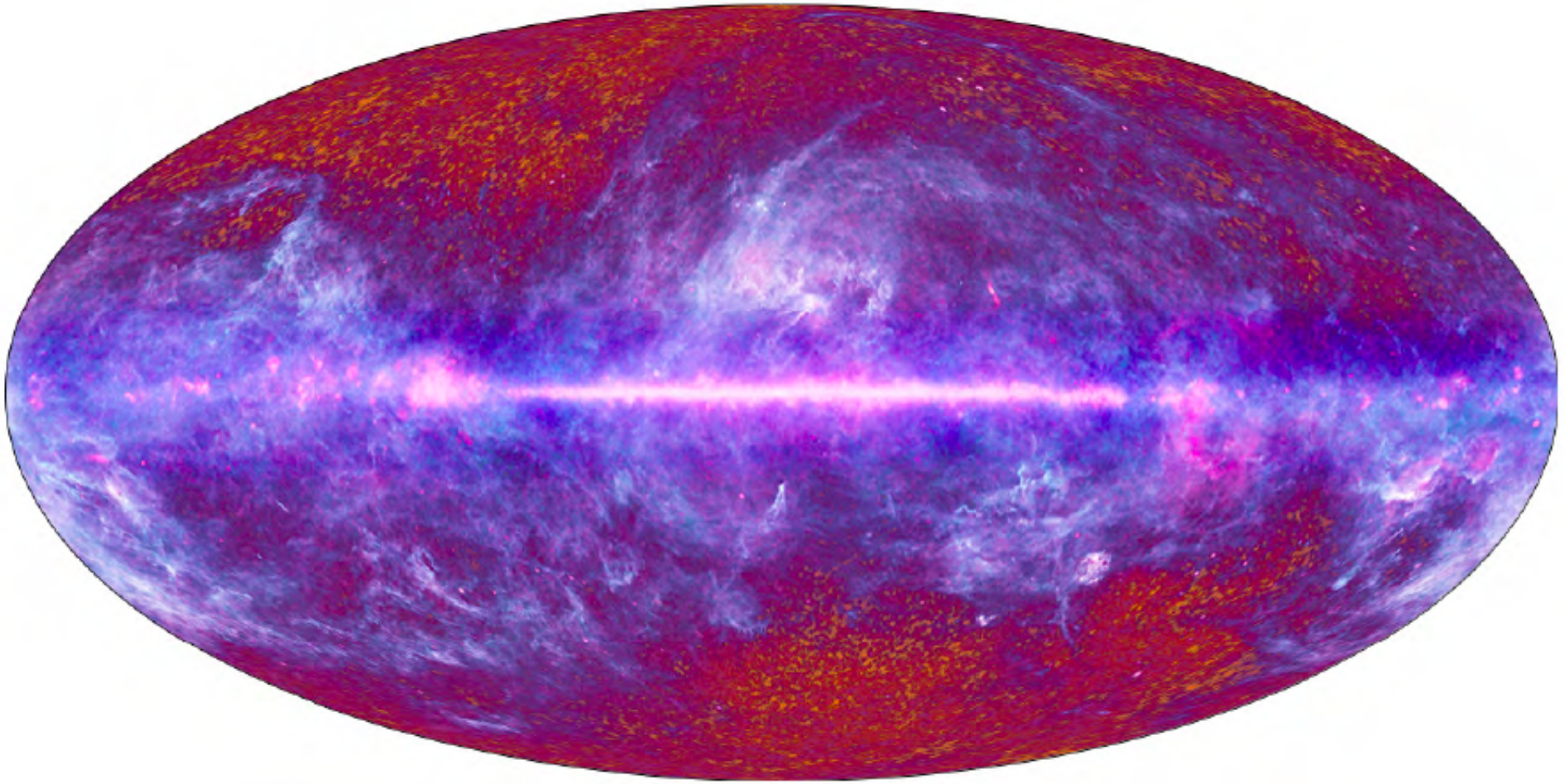

Parameter	*Planck* (CMB+lensing)		*Planck*+WP+highL+BAO	
	Best fit	68 % limits	Best fit	68 % limits
$\Omega_b h^2$	0.022242	0.02217 ± 0.00033	0.022161	0.02214 ± 0.00024
$\Omega_c h^2$	0.11805	0.1186 ± 0.0031	0.11889	0.1187 ± 0.0017
$100\theta_{MC}$	1.04150	1.04141 ± 0.00067	1.04148	1.04147 ± 0.00056
τ	0.0949	0.089 ± 0.032	0.0952	0.092 ± 0.013
n_s	0.9675	0.9635 ± 0.0094	0.9611	0.9608 ± 0.0054
$\ln(10^{10} A_s)$	3.098	3.085 ± 0.057	3.0973	3.091 ± 0.025
Ω_Λ	0.6964	0.693 ± 0.019	0.6914	0.692 ± 0.010
Ω_m	0.3036	0.307 ± 0.019		
σ_8	0.8285	0.823 ± 0.018	0.8288	0.826 ± 0.012
z_{re}	11.45	$10.8^{+3.1}_{-2.5}$	11.52	11.3 ± 1.1
H_0	68.14	67.9 ± 1.5	67.77	67.80 ± 0.77
$10^9 A_s$	2.215	$2.19^{+0.12}_{-0.14}$		
$\Omega_m h^2$	0.14094	0.1414 ± 0.0029		
$\Omega_m h^3$	0.09603	0.09593 ± 0.00058		
Y_P	0.247785	0.24775 ± 0.00014		
Age/Gyr	13.784	13.796 ± 0.058	13.7965	13.798 ± 0.037
z_*	1090.01	1090.16 ± 0.65		
r_*	144.58	144.96 ± 0.66		
$100\theta_*$	1.04164	1.04156 ± 0.00066	1.04163	1.04162 ± 0.00056
z_{drag}	1059.59	1059.43 ± 0.64		
r_{drag}	147.74	147.70 ± 0.63	147.611	147.68 ± 0.45
k_D	0.13998	0.13996 ± 0.00062		
$100\theta_D$	0.161196	0.16129 ± 0.00036		
z_{eq}	3352	3362 ± 69		
$100\theta_{eq}$	0.8224	0.821 ± 0.013		
$r_{drag}/D_V(0.57)$	0.07207	0.0719 ± 0.0011		

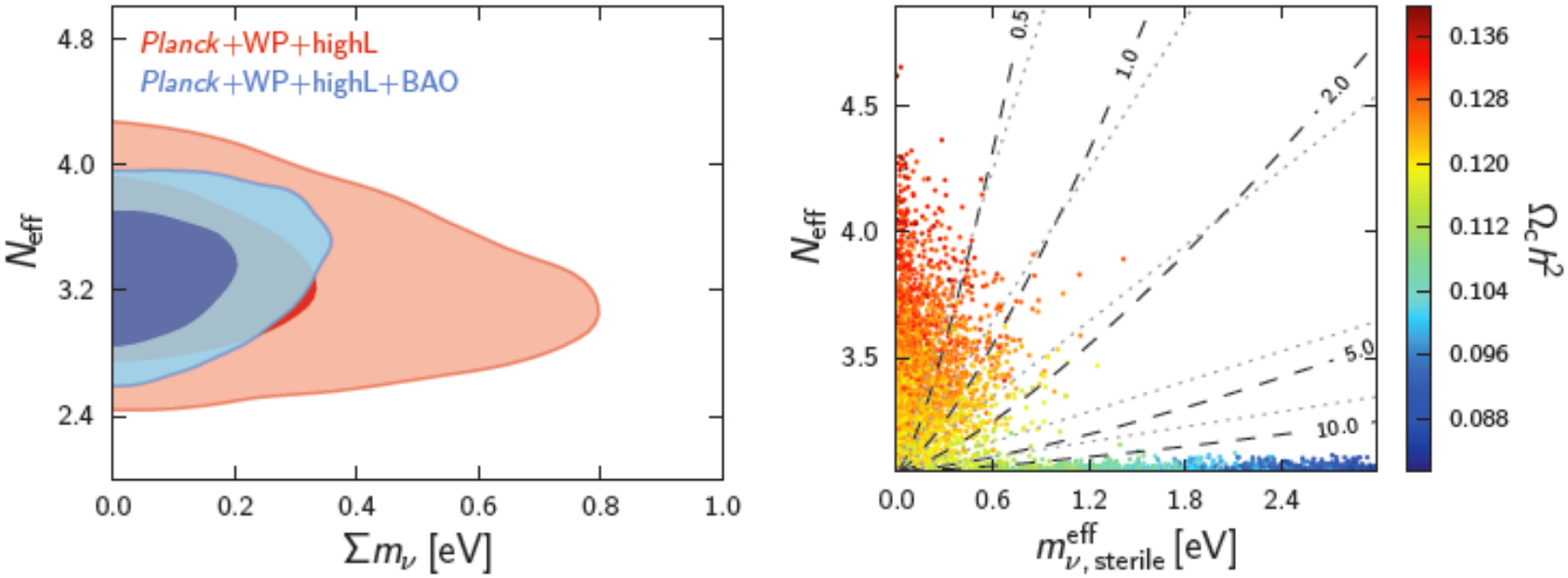

Fig. 28. *Left*: 2D joint posterior distribution between $N_{\rm eff}$ and $\sum m_\nu$ (the summed mass of the three active neutrinos) in models with extra massless neutrino-like species. *Right*: Samples in the $N_{\rm eff}$–$m^{\rm eff}_{\nu,\,\rm sterile}$ plane, colour-coded by $\Omega_c h^2$, in models with one massive sterile neutrino family, with effective mass $m^{\rm eff}_{\nu,\,\rm sterile}$, and the three active neutrinos as in the base ΛCDM model. The physical mass of the sterile neutrino in the thermal scenario, $m^{\rm thermal}_{\rm sterile}$, is constant along the grey dashed lines, with the indicated mass in eV. The physical mass in the Dodelson-Widrow scenario, $m^{\rm DW}_{\rm sterile}$, is constant along the dotted lines (with the value indicated on the adjacent dashed lines).

Cosmology from SZ Cluster Counts (Paper 20)

Planck SZ cluster counts prefer a lower σ_8, lower Ω_m region of the parameter space than the CMB.

… or a modest hydro mass bias and a reasonable neutrino mass!

[in fact a bias similar to that from the maxBCG analysis (2011, A&A, 536, A12)]